

Survey of the Thermodynamic Properties of Hydrazine

Domenico Giordano*

European Space Research & Technology Center, Noordwijk, The Netherlands

The thermodynamic properties of hydrazine in the region of the (T, p) plane covering solid, liquid, and vapor phases have been reviewed and collected for the purpose of validating theoretically derived thermodynamic models of this compound. The data span the time period since 1885 to today, and their characteristics of interest, such as source reliability, numerical accuracy, experimental nature, and so forth, are thoroughly discussed. Unavoidable mistakes, imprecisions, and misinformation that have crept in during the course of the years are pointed out; regions of the (T, p) plane where and properties for which the lack of data is particularly noticeable are appropriately identified.

1. Introductory Considerations

There are many engineering sciences in which the use of hydrazine (N_2H_4) has a role to play, and in most of them, the knowledge of the thermophysical and thermochemical properties of this compound proves to be of utmost importance. In particular, several applications often demand the availability of an N_2H_4 thermodynamic model able to predict analytically the properties of interest. The physically consistent construction of a theoretical model that relies on an assumed empirical state equation $p = p(T, v)$, and other information such as (perfect-gas) constant-pressure heat capacities, is conceptually straightforward [00-gio/des]. On the other hand, physical consistency is a necessary but not sufficient attribute to certify the model for the representation of a real medium: validation tests have to be passed. In other words, analytically predicted thermodynamic properties must satisfactorily compare with values obtained either from direct measurement or from experimentally determined information. Comparison with predictions of other theoretical models may also acquire significance under particular circumstances. It is, therefore, evident that the collection of data into a thermodynamic-property database is a mandatory requisite when embarking in the validation process, and for that matter, one has to rely on what the literature offers. A rich collection of properties is undoubtedly desirable, but which properties in the collection are more significant for the qualification of a model is an important issue that depends on the applications and on the level of generality sought for the model. In this respect, the literature survey presented in this paper took advantage of the recommendations proposed by Martin [59-mar] in 1959 relative to properties of the vapor and liquid phases, which still retain their usefulness today and offer valuable suggestions for the properties of the solid phases, and evolved therefrom. The survey is based on the author's experience gained by reviewing the pertinent literature, spanning the time period since 1885 to today, for the procurement of data necessary to validate a newly developed N_2H_4 thermody-

amic model [00-gio/des] and is offered here for the convenience of other researchers having similar needs. It is the author's opinion that the huge body of references consulted during this work provides a realistic picture of the state-of-the-art relative to the thermodynamic properties for model-validation purposes. Yet, as always when reviewing past works, exhaustiveness is a desired but unreachable asymptote. The reader is, thus, reminded that all statements in this paper touching on data comprehensiveness cannot claim any pretense of absoluteness; they are meant to be understood as relative to the body of references listed herein.

The first studies on N_2H_4 trace back to slightly more than a century ago to the works of Curtius [86-cur/jay, 93-cur, 96-cur], de Bruyn [94-deb, 95-deb, 95-deb-1, 95-deb-2, 96-deb, 99-deb, 02-deb/dit], Brühl [97-bru], and Dito [02-dit, 02-deb/dit]. Since then, several publications have appeared that provide N_2H_4 thermodynamic data and related information. A few of them furnish original experimental data. Others collect and consolidate previously available information as heritage to researchers of future generations; in this regard, the efforts of Audrieth and Ogg [51-aud/ogg] and Schmidt [84-sch] deserve particular mention for the richness and usefulness of their monographs, which, de facto, have become standard references on the subject. Another useful collection is provided by Yaws et al. [74-yaw/hop], who presented the data in the form of graphs. Minor summaries are also available in the handbooks of Kit and Evered [60-kit/eve] and Hannum [85-han]. Unfortunately, unavoidable mistakes, imprecisions, and misinformation have crept in during the inheritance process in the course of the years. They will be appropriately pointed out in the following sections.

The problem of the physical units is inescapable when dealing with the variety featured by the data published over a period of one century. In this work, the data are presented as published, that is, in their original units, to comply with the requirement of passing on trustworthy information and in SI units to adhere to the modern standard. Unit conversion has always been systematically carried out via conversion factors taken from the compilation of Mechtly [73-mec]. Interpolation functions

* To whom correspondence should be addressed. Telephone: + 31 71 565 4392. Fax: + 31 71 565 5421. E-mail: Domenico.Giordano@esa.int.

Table 1. Critical Specific Volume and Compressibility Factor

source	ref	v_c		Z_c
		original data and units	$\times 10^3$ $\text{m}^3 \cdot \text{kg}^{-1}$	
Kit and Evered	60-kit/eve	138.6 ^a $\text{cm}^3 \cdot \text{mol}^{-1}$	4.325	0.3749
Haws and Harden	65-haw/har	1/14.4 $\text{ft}^3 \cdot \text{lbm}^{-1}$	4.335	0.3758
Das and Kuloor	68-das/kul	0.1389 ^a $\text{L} \cdot \text{mol}^{-1}$	4.334	0.3757
Yaws et al.	74-yaw/hop	101.1 ^a $\text{cm}^3 \cdot \text{mol}^{-1}$	3.155	0.2735
Hannum	85-han	1/0.2313 $\text{m}^3 \cdot \text{Mg}^{-1}$	4.323	0.3748

^a Molar specific volume; divide by molar mass (32.045 282 $\times 10^{-3}$ $\text{kg} \cdot \text{mol}^{-1}$) for conversion.

are faithfully reported as published in the original references.

2. Liquid–Vapor Saturation Curve

A. Critical Data. The experimental determination of the critical temperature was carried out by de Bruyn [96-deb] in 1896. In a series of two distinct experiments he found $t_c = 380$ °C (653.15 K) and $t_c = 355$ °C (628.15 K). De Bruyn [96-deb] also reported the experimental critical pressure $p_c = (145 \pm 0.3)$ atm (14.69 MPa) measured by Boltwood in the laboratory directed by Ostwald in Leipzig (Germany). Although no explicit bibliographic reference is given, de Bruyn provides an accurate account of Boltwood's experiment. The critical pressure and the first value of the critical temperature have been consistently reported in subsequent publications [33-wes/hul, 51-aud/ogg, 60-kit/eve, 65-haw/har, 68-das/kul, 74-yaw/hop, 84-sch, 85-han, 87-rei/pra]. For the sake of the record, however, it ought to be remarked that the second value measured for the critical temperature has never been mentioned in the literature. Moreover, de Bruyn's warnings about the appearance in his experiments of N_2H_4 decomposition [92-bel] in the vicinity of its critical point cast some doubts [51-aud/ogg, 84-sch] about the accuracy of these data.

The critical specific volume (or density) does not lend itself to easy experimental determination [59-mar]. A few values available in the literature are summarized in Table 1 together with the corresponding critical compressibility factor $Z_c = p_c v_c M R T_c$, based on the above critical pressure and temperature (first value). No information is given by the authors listed in Table 1 regarding the origin of the data they propose, with the exception of Yaws et al. [74-yaw/hop], who declared their estimate based on a method attributed to Herzog [44-her]. A certain agreement among the data is evident, although the compressibility factors are suspiciously near $Z_c = 0.375 = 3/8$ of the van der Waals model. This coincidence might support the conjecture that the specific-volume data could have been derived from the a priori assumption that $Z_c = 3/8$ for N_2H_4 , together with the critical temperature and pressure indicated by de Bruyn. Yaws et al., however, obtained a significantly lower specific volume which yields a compressibility factor complying with the rule of thumb expressed by Martin [59-mar], according to whom: "For most compounds Z_c will lie between 0.25 and 0.28. If it does not, either the compound is unusual or the data are in error".

The values of p_c , T_c , and v_c assumed in this work for the purpose, and only for that, of representing nondimensional variables are respectively 14.69 MPa, 653.15 K, and 4.335×10^{-3} $\text{m}^3 \cdot \text{kg}^{-1}$; by definition, the reciprocal of the latter figure represents the critical density.

B. Vapor Pressure of Liquid N_2H_4 . The vapor pressure of liquid N_2H_4 is undoubtedly the best experimentally

Table 2. Liquid N_2H_4 Vapor Pressure Measured by de Bruyn in 1895–6

ref	original units		SI units	
	$t/^\circ\text{C}$	p_v/mmHg	T/K	p_v/Pa
95-deb-2	56.0	71.0	329.15	9.466×10^3
95-deb-2	113.5 ^a	761.0	386.65	1.015×10^5
96-deb	113.5 ^a	761.5	386.65	1.015×10^5
96-deb	134.6	1490.0	407.75	1.987×10^5
96-deb	380.0 ^b	110200.0 ^c	653.15	1.469×10^7

^a Normal boiling point. ^b Critical point. ^c Converted from $p_c = 145$ atm (see section 2.A).

Table 3. Liquid N_2H_4 Vapor Pressure Data Incorrectly Claimed to de Bruyn's Experimental Investigations [95-deb-2, 96-deb] in the *International Critical Tables* [33-wes/hul]

$t/^\circ\text{C}$	original units		SI units	
	p_v/atm	T/K	p_v/Pa	
140	2.3	413.15	2.330×10^5	
170	5	443.15	5.066×10^5	
200	10	473.15	1.013×10^6	
250	26	523.15	2.634×10^6	
300	56	573.15	5.674×10^6	
350	104	623.15	1.054×10^7	

investigated property of this compound. The earliest measurements were carried out by de Bruyn [95-deb-2, 96-deb] during the last decade of the past century, and his experimental data, summarized in Table 2, have been reported in [33-wes/hul, 51-aud/ogg, 65-haw/har]. There exist other data (see Table 3) tabulated in the *International Critical Tables* [33-wes/hul], and subsequently trusted by Audrieth and Ogg [51-aud/ogg] and Haws and Harden [65-haw/har], which are claimed as having been published by de Bruyn in [95-deb-2, 96-deb]. Unfortunately, the information provided by the *International Critical Tables* appears to be incorrect because repeated and careful inspection of not only [95-deb-2, 96-deb] but all de Bruyn's publications on N_2H_4 reveals no trace of the data in question. One has to conclude, therefore, that, although the data (solid squares in Figure 1) seem to fit consistently between those (hollow squares in Figure 1) of Table 2, their origin and experimental nature are unknown.

According to Schmidt [84-sch], the data in Tables 2 and 3 constitute all that is available above the normal boiling point (NBP). The situation at and below the NBP is more favorably disposed (see Figure 1). NBP data published in the literature [96-cur, 34-hie/woe, 38-sem, 39-fre/kar, 41-gig, 52-bur, 63-pan/mig, 85-han, 87-rei/pra] are shown in Table 4 together with the findings of de Bruyn's early investigations and are seen to agree within very minor differences. Below the NBP, vapor pressure measurements have been carried out by Hieber and Woerner [34-hie/woe], Fresenius and Karweil [39-fre/kar], Scott et al. [49-sco/oli], Burtle [52-bur], and Chang and Gokcen [64-cha/gok]. Hannum [85-han] also published vapor pressure values, the experimental nature of which, however, is difficult to ascertain. Data published in tabular form [34-hie/woe, 49-sco/oli, 52-bur, 64-cha/gok, 85-han] are reproduced in Tables 5–9 and are compared in Figure 1; the agreement among the data is quite satisfactory, although minor differences exist and are traceable [84-sch] mainly to the differences in purity of the N_2H_4 samples used by the various experimenters. Fresenius and Karweil did not tabulate their experimental data but reported them only in the form of a graph, the scanner reproduction of which is shown in Figure 2a; unfortunately, accurate comparison

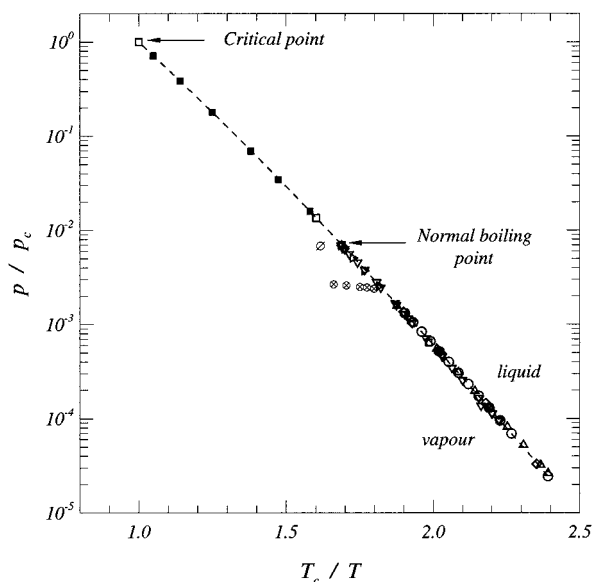


Figure 1. Vapor pressure of liquid N_2H_4 : \square , de Bruyn [95-deb-2, 96-deb]; \blacksquare , *International Critical Tables* [33-wes/hul] (erroneously claimed to de Bruyn); ∇ , Hieber and Woerner [34-hie/woe]; \circ , Scott et al. [49-sco/oli]; right triangle, Burtle [52-bur]; \triangle , Chang and Gokcen [64-cha/gok]; \diamond , Hannum [85-han]; ---, interpolation (eq 1) by Das and Kuloor [68-das/kul]. The pressure–volume–temperature experimental data of Giguere and Rundle [41-gig/run] relative to nonsaturated vapor are also superposed (\otimes , $\rho/\rho_c = 1.583 \times 10^{-3}$; \emptyset , $\rho/\rho_c = 4.120 \times 10^{-3}$).

Table 4. Normal Boiling Point at $p_v = 760$ mmHg (1.01325×10^5 Pa)

source	ref	original units		SI units	
		$t/^\circ\text{C}$	T/K	$t/^\circ\text{C}$	T/K
de Bruyn	95-deb-2	113.50 ^a	386.65		
Curtius	96-cur	113.50 ^b	386.65		
de Bruyn	96-deb	113.50 ^c	386.65		
Hieber and Woerner	34-hie/woe	114.15	387.30		
Semishin	38-sem	113.50 ^d	386.65		
Fresenius and Karweil	39-fre/kar	113.40	386.55		
Giguere	41-gig	113.50 ^b	386.65		
Burtle	52-bur	113.80 ^e	386.95		
Pannetier and Mignotte	63-pan/mig	113.00 ^f	386.15		
Hannum	85-han	113.65	386.80 ^g		
Reid et al.	87-rei/pra	113.55 ^b	386.70 ^g		

^a $p_v = 761$ mmHg (1.01458×10^5 Pa). ^b Pressure not explicitly mentioned in referenced source. ^c $p_v = 761.5$ mmHg (1.01525×10^5 Pa). ^d Taken from Audrieth and Ogg [51-aud/ogg]. ^e Extrapolated. ^f From curve labeled “ $P = 760$ mm” in Figure 1 of the original reference. ^g Original units. Converted to $^\circ\text{C}$ in third column.

with the data listed in Tables 5–8 is impaired because the graph is not detailed enough to permit reliable determination of numerical values. Nevertheless, the evident similarity between parts a and b of Figure 2, with the latter part showing the data of Tables 5–8 adapted to the style of Figure 2a, indicates that, at least qualitatively, the experimental findings of Fresenius and Karweil are substantially in accordance with those of Hieber and Woerner, Scott et al., Burtle, and Chang and Gokcen. Concerning the latter authors, it may be of interest to point out some inaccuracies present in Table 3 of [64-cha/gok], reproduced here in Table 10, where Chang and Gokcen confront some of their experimental data, marked with superscript ‘b’ in Table 8, with data they attributed to Hieber and Woerner, Scott et al., and Pannetier and Mignotte [63-pan/mig]. With reference to Table 10, the values in the third column and

Table 5. Liquid N_2H_4 Vapor Pressure Measured by Hieber and Woerner [34-hie/woe]

original units		SI units	
$t/^\circ\text{C}$	p_v/mmHg	T/K	p_v/Pa
20.21	10.4*	293.36	1.387×10^3
20.60	10.7	293.75	1.427×10^3
23.67	12.4	296.82	1.653×10^3
23.73	12.6	296.88	1.680×10^3
26.02	14.6*	299.17	1.947×10^3
28.84	15.1	301.99	2.013×10^3
29.85	18.3	303.00	2.440×10^3
37.89	28.2	311.04	3.760×10^3
43.32	38.1	316.47	5.080×10^3
48.48	50.3	321.63	6.706×10^3
48.60	50.8	321.75	6.773×10^3
57.41	78.1	330.56	1.041×10^4
65.63	114.0	338.78	1.520×10^4
67.82	127.3	340.97	1.697×10^4
70.04	141.7	343.19	1.889×10^4
75.27	176.2	348.42	2.349×10^4
76.01	184.2	349.16	2.456×10^4
85.38	271.0	358.53	3.613×10^4
88.20	308.8*	361.35	4.117×10^4
96.43	417.1	369.58	5.561×10^4
101.66	502.2	374.81	6.695×10^4
107.85	615.9	381.00	8.211×10^4
111.33	696.2	384.48	9.282×10^4
114.15 ^a	760.0*	387.30	1.013×10^5

^a Normal boiling point.

Table 6. Liquid N_2H_4 Vapor Pressure^a Measured by Scott et al. [49-sco/oli]

original units		SI units	
$t/^\circ\text{C}$	p_v/mmHg	T/K	p_v/Pa
0	2.69 ^b	273.15	3.586×10^2
15	7.65	288.15	1.020×10^3
20	10.55	293.15	1.407×10^3
25	14.38	298.15	1.917×10^3
30	19.29	303.15	2.572×10^3
35	25.67	308.15	3.422×10^3
40	33.82	313.15	4.509×10^3
45	44.08	318.15	5.877×10^3
50	56.91	323.15	7.587×10^3
55	72.85	328.15	9.713×10^3
60	92.43	333.15	1.232×10^4
65	116.30	338.15	1.551×10^4
70	145.12	343.15	1.935×10^4

^a Series III of experiments from Table 2 of [49-sco/oli]. ^b Supercooled liquid.

Table 7. Liquid N_2H_4 Vapor Pressure Measured by Burtle [52-bur]

% $\text{N}_2\text{H}_4/\text{mol}$	original units		SI units	
	$t/^\circ\text{C}$	p_v/mmHg	T/K	p_v/Pa
98.95	66.8	124.8	339.95	1.664×10^4
98.76	86.5	281.8	359.65	3.757×10^4
98.06	96.8	411.2	369.95	5.482×10^4
97.37	105.2	560.4	378.35	7.471×10^4
97.87	111.7	700.6	384.85	9.341×10^4
-	113.8 ^a	760.0	386.95	1.013×10^5

^a Extrapolated normal boiling point.

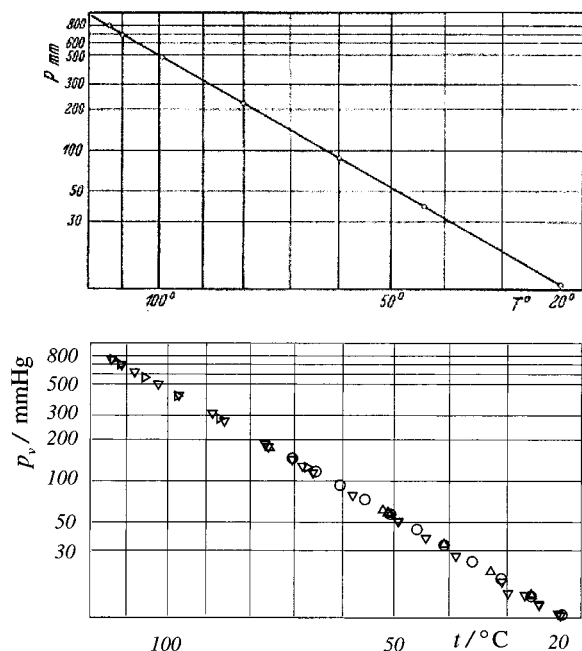
the value at the bottom row of the fourth column do not appear in [34-hie/woe, 49-sco/oli] respectively, as it is readily seen from inspection of Tables 5 and 6. On the other hand, it is not clear from Chang and Gokcen’s text if these data were directly taken from the references they cite or were the outcome of interpolation or a curve-fitting process. Concerning the values in the fifth column attributed to Pannetier and Mignotte, it ought to be said that these

Table 8. Liquid N₂H₄ Vapor Pressure^a Measured by Chang and Gokcen [64-cha/gok]

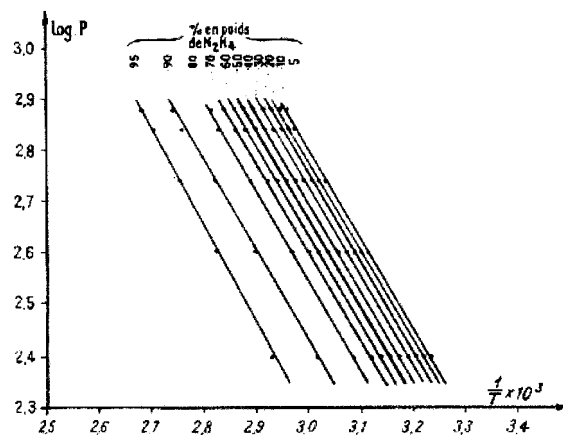
original units		SI units	
<i>t</i> /°C	<i>p_v</i> /mmHg	<i>T</i> /K	<i>p_v</i> /Pa
0.00	2.90 ^b	273.15	3.866 × 10 ²
2.90	3.56	276.05	4.746 × 10 ²
9.90	5.78	283.05	7.706 × 10 ²
16.80	9.04	289.95	1.205 × 10 ³
24.86	14.46	298.01	1.928 × 10 ³
25.00	14.79 ^b	298.15	1.972 × 10 ³
31.80	21.71	304.95	2.894 × 10 ³
40.00	34.32	313.15	4.576 × 10 ³
50.00	56.61 ^b	323.15	7.547 × 10 ³
50.47	57.84	323.62	7.711 × 10 ³
50.48	58.28	323.63	7.770 × 10 ³
51.47	60.75	324.62	8.099 × 10 ³
75.00	173.30 ^b	348.15	2.310 × 10 ⁴

^a From Table 2 of [64-cha/gok], unless otherwise indicated.^b From Table 3 of [64-cha/gok].**Table 9. Liquid N₂H₄ Vapor Pressure Reported by Hannum [85-han]^a**

<i>T</i> /K	<i>p_v</i> /Pa
277.6	4.830 × 10 ²
298.0	1.920 × 10 ³
299.8	2.140 × 10 ³
322.0	7.170 × 10 ³
344.0	2.000 × 10 ⁴
386.8 ^b	1.013 × 10 ⁵ ^c

^a The experimental nature of the data could not be ascertained.^b Normal boiling point. ^c Converted from *p_v* = 760 Torr.**Figure 2.** Comparison (a, top) the experimental vapor pressure curve of liquid N₂H₄ from Fresenius and Karweil [39-fre/kar] (scanner reproduction of Figure 1 in the original reference) and (b, bottom) corresponding data from other authors (Tables 5–8 respectively): ▽, Hieber and Woerner [34-hie/woe]; ○, Scott et al. [49-sco/oli]; right triangle, Burtle [52-bur]; △, Chang and Gokcen [64-cha/gok].

authors have carried out experimental investigations of mixtures composed of N₂H₄ and unsymmetrical dimethylhydrazine (UDMH), and the mixture nearest to pure N₂H₄ considered in their study contained 95 mass % N₂H₄ and 5 mass % UDMH. Pannetier and Mignotte presented their experimental findings in graphical form. The scanner

**Figure 3.** Experimental vapor pressure curves of hydrazine–dimethylhydrazine mixtures from Pannetier and Mignotte [63-pan/mig] (scanner reproduction of Figure 4 in the original reference).**Table 10. Comparative Table of Experimental Vapor Pressure Data of Liquid N₂H₄ from Chang and Gokcen [64-cha/gok] (Reproduction of Table 3 in the Original Reference)**

<i>t</i> /°C	<i>p_v</i> /mmHg			
	Chang and Gokcen	Hieber and Woerner	Scott et al.	Pannetier and Mignotte
0	2.90	2.67	2.69	2.83
25	14.79	13.75	14.38	14.13
50	56.61	54.60	56.91	54.83
75	173.3	175.5	179.9	175.4

reproduction of their vapor pressure graph is shown in Figure 3. It evidences the high sensitivity of the vapor pressure curve to the mixture composition when the latter approaches pure N₂H₄. Chang and Gokcen's extrapolation is based on the interpolation formula $\log_{10} p_v/\text{mmHg} = -(2272/T) + 8.770$ derived by them after careful scaling of Pannetier and Mignotte's curves. However, they do not provide detailed information regarding how the extrapolation of the vapor pressure line toward pure N₂H₄ is accomplished in terms of the mixture composition.

The necessity to have the vapor pressure curve available in analytical form to perform thermodynamic calculations has promoted the proliferation of interpolating functions [33-wes/hul, 34-hie/woe, 49-sco/oli, 51-aud/ogg, 64-cha/gok, 65-haw/har, 68-das/kul, 84-sch] that fit vapor pressure data in specified temperature ranges. These interpolating functions are, in general, sufficiently accurate; in particular, the expression proposed by Das and Kuloor [68-das/kul]

$$\ln p_v/\text{atm} = 58.7582 - \frac{0.707 \times 10^4}{T} - 7.088 \ln T + (0.457 \times 10^{-2}) T \quad (1)$$

appears to be the most remarkable one because it accurately reproduces (dashed line in Figure 1) the experimental data from 0 °C (273.15 K) to 380 °C (653.15 K), that is, up to the critical point. On the other hand, readers are warned that the interpolating function

$$\ln p_v/\text{psia} = 24.24 - [18184.9/(T/R)] + 0.47629 \ln(T/R) - 0.003836(T/R) + \{1115.43[1190.08 - (T/R)]/1190.088\} \ln[1190.08 - (T/R)] \quad (2)$$

published by Haws and Harden [65-haw/har] and reported also by Schmidt [84-sch], fails completely in reproducing the experimental data, notwithstanding the (somewhat

Table 11. Data Reported as Saturated-Liquid Density by Haws and Harden [65-haw/har]^a

original units		SI units	
$t/^\circ\text{F}$	$\rho_l/(\text{lbm}\cdot\text{ft}^{-3})$	T/K	$\rho_l/(\text{kg}\cdot\text{m}^{-3})$
32.0	63.90*	273.15	1023.6
68.0	62.90*	293.15	1007.6
95.0	62.15*	308.15	995.5
260.6	57.30	400.15	917.9
322.6	52.98	434.59	848.7
404.6	48.04	480.15	769.5
476.6	42.80	520.15	685.6
548.6	37.10	560.15	594.3
620.6	30.50	600.15	488.6
692.6	21.80	640.15	349.2

^aData marked with an asterisk were published as *liquid densities* by Audrieth and Ogg [51-aud/ogg]. The origin of the unmarked data is unknown.

puzzling) supporting comparative Table 1 given in [65-haw/har]; in particular, the factor between the braces in eq 2 becomes unreasonably too big for exponentiation when $T \rightarrow 491.67 \text{ R}$ (273.15 K). In the same guise, a systematic error affects the interpolating function

$$\log_{10} p_v/\text{mmHg} = 9.40 - \frac{2814.9}{T} - 0.006931 T + 0.000003746 T^2 \quad (3)$$

given by Audrieth and Ogg [51-aud/ogg] for temperatures above the NBP. The correct values are recovered by adding the factor $\log_{10} 760 \approx 2.881$ to the right-hand side of eq 3.

C. Saturated-Liquid and -Vapor Specific Volumes (or Densities). The saturated-liquid and -vapor specific volumes (or densities) are among the most poorly investigated properties of N_2H_4 . To the best of the author's findings in the literature, only a few researchers have touched upon [60-kit/eve] or dealt with [65-haw/har, 68-das/kul] these properties, and they all share the following characteristic: the claim of correspondence to saturation conditions of the experimental and/or calculated data they referenced and reported turns out to be unfounded. It can, thus, be maintained that no direct experimental determination of the properties in question has ever been attempted. The mentioned characteristic may trigger a mild concern for the liquid phase because the weak variability of the corresponding specific volume with pressure $\{v(T,p) \approx v[T,p_v(T)]\}$ would presuppose the introduction of a negligible numerical error, at least sufficiently away from the critical-point neighborhood. Of course, the vapor phase would require more attention. Yet, this apparently harmless matter acquires importance when viewed with the target in mind of validating a thermodynamic model because the theoretical methods to compute saturated- and nonsaturated-phase properties are radically different. It is always a sane habit to proceed with physically consistent data or, at least, to be aware of the hidden inconsistencies affecting them. With concern to the latter aspect, Kit and Evered [60-kit/eve] have incorrectly labeled as saturated the vapor whose density was calculated by them from the experimentally determined pressure–volume–temperature data of Giguere and Rundle [41-gig/run] (see Section 5), which, as illustrated in Figure 1, are readily checked not to fall on the saturation curve. Similarly, Haws and Harden [65-haw/har] have published *saturated-liquid density* data, tabulated in Table 11 and plotted in Figure 4, which they claimed are taken from the compilation of Audrieth and Ogg [51-aud/ogg]. However, the latter authors manifestly declared as liquid density the data contained in their

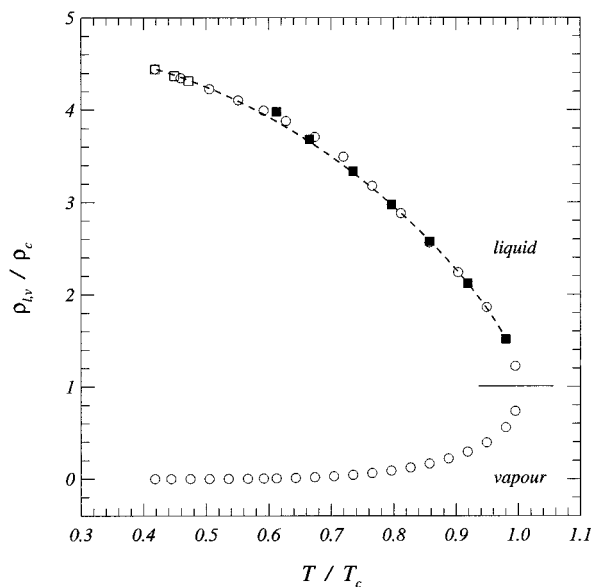


Figure 4. Saturated-liquid density values proposed by Haws and Harden [65-haw/har] but inaccurately claimed to Audrieth and Ogg [51-aud/ogg] (□, declared as *liquid density* by Audrieth and Ogg; ■, unknown origin because not present in Audrieth and Ogg's tabulation; — —, interpolation (eq 4) by Haws and Harden) and saturated-liquid and -vapor densities estimated by Das and Kuloor [68-das/kul] (○).

Table 12. Saturated-Liquid and -Vapor Molar Specific Volumes Estimated by Das and Kuloor [68-das/kul]

T	Mv_l	Mv_v	T	Mv_l	Mv_v
K	$\text{L}\cdot\text{mol}^{-1}$	$\text{L}\cdot\text{mol}^{-1}$	K	$\text{L}\cdot\text{mol}^{-1}$	$\text{L}\cdot\text{mol}^{-1}$
273.16	0.031 26	6367.0	460	0.038 90	4.72
280	0.031 43	3981.3	470	0.039 77	3.84
290	0.031 69	2105.3	480	0.040 83	3.16
300	0.031 97	1166.2	490	0.042 33	2.62
310	0.032 27	677.9	500	0.043 72	2.18
320	0.032 57	411.2	510	0.045 26	1.84
330	0.032 87	258.2	520	0.046 70	1.55
340	0.033 19	167.5	530	0.048 20	1.32
350	0.033 51	111.9	540	0.049 94	1.13
360	0.033 84	76.79	550	0.051 90	0.973
370	0.034 17	53.95	560	0.054 20	0.839
380	0.034 54	38.86	570	0.056 40	0.726
386.66	0.034 78	31.46	580	0.059 10	0.629
390	0.034 94	28.51	590	0.062 00	0.546
400	0.035 34	20.96	600	0.065 60	0.473
410	0.035 80	15.77	610	0.069 6	0.405
420	0.036 29	12.07	620	0.074 6	0.352
430	0.036 84	9.37	630	0.081 2	0.299
440	0.037 47	7.37	640	0.091 6	0.249
450	0.038 15	5.87	650	0.113 5	0.189

collection (see Section 5); furthermore, apart the property mismatch, additional uncertainty is introduced by the discovery that only the data marked with an asterisk in Table 11 (hollow squares in Figure 4 and footnote 'b' in Table 18) are present in Audrieth and Ogg's list. This fact leads to draw the obvious, although negative, conclusion that the unmarked data (solid squares in Figure 4) have an unknown origin and nature; it is, therefore, impossible to ascertain their reliability. At any rate, Haws and Harden have fitted the values in the second column of Table 11 and have provided the following interpolation function

$$\rho_l/(\text{lbm}\cdot\text{ft}^{-3}) = 14.4 + 86.820(1 - \tau) + 6.3431(1 - \tau)^{1/2} + 17.716(1 - \tau)^{1/3} - 60.654(1 - \tau)^2 \quad (4)$$

for the purpose of analytical calculations. In eq 4, $\tau = T/T_c$

Table 13. Molar Vaporization Enthalpy Estimated by Various Authors

source	ref	original units		SI units	
		<i>t</i> °C	$\Delta_{\text{vap}}H$ kcal·mol ⁻¹	<i>T</i> K	$\Delta_{\text{vap}}H$ J·mol ⁻¹
Hieber and Woerner	34-hie/woe	23.1	10.20	296.25	42 705
		101.0	9.67	374.15	40 486
Fresenius and Karweil	39-fre/kar	20.0	10.00 ^a	293.15	41 868
		↓		↓	
		113.5		386.65	
Giguere	41-gig	113.5	9.60	386.65	40 193
Scott et al.	49-sco/oli	25.0	10.70 ^{a,b}	298.15 ^c	44 799
Schmidt	84-sch	25.0	10.38	298.15 ^c	43 459
		114.2	9.34	387.35 ^c	39 105

^a Original units in cal·mol⁻¹. ^b Within estimated uncertainty of ±0.075 kcal·mol⁻¹ (314 J·mol⁻¹). ^c Original units. Converted to °C in third column.

Table 14. Molar Vaporization Enthalpy Estimated by Das and Kuloor [68-das/kul]

original units		SI units	original units		SI units
<i>T</i> K	$\Delta_{\text{vap}}H$ cal·mol ⁻¹	$\Delta_{\text{vap}}H$ J·mol ⁻¹	<i>T</i> K	$\Delta_{\text{vap}}H$ cal·mol ⁻¹	$\Delta_{\text{vap}}H$ J·mol ⁻¹
273.16	10 866.3	45 495.0	460	9 043.6	37 864
280	10 810.8	45 262.7	470	8 887.7	37 211
290	10 730.0	44 924.4	480	8 745.6	36 616
300	10 647.0	44 576.9	490	8 579.9	35 922
310	10 555.5	44 193.8	500	8 380.0	35 085
320	10 476.8	43 864.3	510	8 221.2	34 421
330	10 401.6	43 549.4	520	7 987.2	33 441
340	10 315.6	43 189.4	530	7 791.0	32 619
350	10 244.5	42 891.7	540	7 570.8	31 697
360	10 170.0	42 579.8	550	7 359.0	30 811
370	10 093.6	42 259.9	560	7 095.2	29 706
380	10 013.0	41 922.4	570	6 828.6	28 590
386.66	9 956.5	41 686	580	6 519.2	27 295
390	9 933.3	41 589	590	6 189.1	25 913
400	9 828.0	41 148	600	5 808.0	24 317
410	9 733.4	40 752	610	5 368.0	22 475
420	9 613.8	40 251	620	4 854.6	20 325
430	9 481.5	39 697	630	4 208.4	17 620
440	9 345.6	39 128	640	3 353.6	14 041
450	9 202.5	38 529	650	1 768.0	7 402

is the reduced temperature and the constant term on the right-hand side represents the critical density (see Table 1 and Section 2.A). Equation 4 has been reported also by Schmidt [84-sch]; its satisfactory performance is illustrated by the dashed line in Figure 4. Das and Kuloor [68-das/kul] also incurred the same kind of misinterpretations outlined above. Concerning the vapor phase, they complemented the already mentioned Giguere and Rundle's pressure–volume–temperature data with a calculation of the saturated-vapor specific volume based on the combination of eq 1 with a virial-expansion state equation particularized to N₂H₄ from a generic theoretical model proposed by Martin and co-workers [55-mar/hou, 59-mar/kap]. Concerning the liquid phase, they trusted the previously discussed Haws and Harden's data and used the liquid-density data given by Ahlert et al. [62-ahl/bau] (see Section 5 and footnote 'd' in Table 18). The simultaneous curve fit of the various sets of values, for both liquid and vapor phases, respectively, produced the results shown in Table 12. The latter have been rearranged in terms of densities and plotted in Figure 4; as expected, figures compare well with those of Haws and Harden for the liquid phase.

In connection with the calculation method used by Das and Kuloor for the saturated-vapor specific volume, it appears relevant to raise a warning against the practice to combine arbitrary state equations $p = p(T, \nu)$ with

Table 15. Normal Melting Point

source	ref	original units	SI units
		<i>t</i> /°C	<i>T</i> /K
de Bruyn	95-deb-1	2	275.15
	95-deb-2	1.4	274.55
Curtius	96-cur	2	275.15
de Bruyn	96-deb	1.4	274.55
Friedrichs	23-fri	1.8 ^a	274.95
Hieber and Woerner	34-hie/woe	1.4	274.55
Semishin	38-sem	1.6 → 1.7 ^a	274.75 → 274.85
Fresenius and Karweil	39-fre/kar	1 → 2	274.15 → 275.15
Pleskov	40-ple	1.85 ^a	275.00
Giguere	41-gig	1.7	274.85
Scott et al.	49-sco/oli	1.41	274.56 ^{b,c}
		1.54	274.69 ^{b,d}
Mohr and Audrieth	49-moh/aud	2.0 ^a	275.15
Williams	73-wil	1.505	274.655 ^{b,e}
Litvinova et al.	78-lit/mis	2.2	275.35 ^{b,e}
Hannum	85-han	1.85	275 ^b
Reid et al.	87-rei/pra	1.55	274.7 ^b

^a Taken from Audrieth and Ogg [51-aud/ogg]. ^b Original units. Converted to °C in third column. ^c Measured on the actual 99.75% sample. ^d Calculated for the pure material. ^e Taken from Schmidt [84-sch].

Table 16. Experimental Freezing Point versus Pressure Measured by Hoffman [76-hof]

original units		SI units	
<i>t</i> /°F	<i>p</i> /psia	<i>T</i> /K	10 ⁻⁷ <i>p</i> /Pa
30.4 ^a	14.7	272.26	0.010
30.5 ^a	14.7	272.32	0.010
33.8	3000	274.15	2.068
33.9	3000	274.21	2.068
34.2	3000	274.37	2.068
37.3	6000	276.09	4.137
37.4	6000	276.15	4.137
37.6	6000	276.26	4.137
39.0	8000	277.04	5.516
39.4	8000	277.26	5.516
39.6	8000	277.37	5.516

^a Normal melting point?

Table 17. Molar Enthalpy of Fusion Estimated by Various Authors

source	ref	original units		SI units	
		<i>t</i> °C	$\Delta_{\text{fus}}H$ cal·mol ⁻¹	<i>T</i> K	$\Delta_{\text{fus}}H$ J·mol ⁻¹
Hieber and Woerner	34-hie/woe	1.4	1020 ^a	274.55	4271
Giguere	41-gig	1.7	1000 ^a	274.85	4187
Scott et al.	49-sco/oli	1.41	3025	274.56 ^b	12665
Kit and Evered	60-kit/eve	25.0	94.5 ^c	298.15	12679

^a Original units in kcal·mol⁻¹. ^b Original units. Converted to °C in third column. ^c Enthalpy of fusion per unit mass. Multiply by molar mass (32.045 282 × 10⁻³ kg·mol⁻¹) for conversion.

interpolating functions $p_v^{\text{int}}(T)$ of experimental vapor pressure data for the purpose of obtaining saturated-liquid and -vapor specific volumes. Such a practice should be discouraged for the following very important reason: the assignment of a theoretical state equation implies the existence of a corresponding theoretical function $p_v^{\text{the}}(T)$ which does not necessarily match the experimental data that the selected function $p_v^{\text{int}}(T)$ interpolates [00-gio/des]. In other words, the unsubstantiated adoption of an arbitrary state

Table 18. Liquid Density Data Measured by Various Authors

source	ref	original units		SI units	
		<i>t</i>	ρ	<i>T</i>	$10^{-3}\rho$
		°C	g·cm ⁻³	K	kg·m ⁻³
de Bruyn	96-deb	15	1.014	288.15	1.014
	95-deb-1	23	1.0075	296.15	1.0075
	95-deb-2	23	1.003	296.15	1.003
Brühl ^a	97-bru	0	1.0258	273.15	1.0258
		0.2	1.0256	273.35	1.0256
		20	1.0085 ^b	293.15	1.0085
		22.3	1.0065	295.45	1.0065
Dito	02-dit	15	1.0114	288.15	1.0114
Walden and Hilgert ^a	33-wal/hil	0	1.0253	273.15	1.0253
		15	1.0140	288.15	1.0140
		25	1.0045	298.15	1.0045
		25	1.0036	298.15	1.0036
Barrick et al. ^a	36-bar/dra	35	0.9955 ^b	308.15	0.9955
	Semishin ^a	38-sem	0	1.0231 ^b	273.15
25		1.0024	298.15	1.0024	
50		0.9801	323.15	0.9801	
Hough et al.	50-hou/mas	0	0.9816	273.15	0.9816
		50	0.9780	323.15	0.9780
Kretschmar	53-kre	25	1.0096 ^c	298.15	1.0096
	54-kre	25	1.004	298.15	1.004
Ahlert et al. ^d	62-ahl/bau	23.09	1.0059	296.24	1.0059
		26.60	1.0026	299.75	1.0026
		37.11	0.9942	310.26	0.9942
		37.11	0.9946	310.26	0.9946
		37.11	0.9930	310.26	0.9930
		37.11	0.9931	310.26	0.9931
		65.58	0.9672	338.73	0.9672
		65.58	0.9671	338.73	0.9671
		93.34	0.9388	366.49	0.9388
		93.34	0.9398	366.49	0.9398
		93.34	0.9391	366.49	0.9391
121.12	0.9124	394.27	0.9124		
148.90	0.8862	422.05	0.8862		
148.89	0.8863	422.04	0.8863		
176.68	0.8573	449.83	0.8573		
176.68	0.8577	449.83	0.8577		
Hannum ^d	85-han	19.85	1.008	293	1.008
Laachach et al. ^d	92-laa/fer	5.00	1.0305	278.15	1.0305
		20.00	1.0140	293.15	1.0140

^a Data taken from Audrieth and Ogg [51-aud/ogg]. ^b Taken by Haws and Harden [65-haw/har] from the compilation of Audrieth and Ogg [51-aud/ogg] and used as *saturated-liquid density*; data correspond to those marked with an asterisk in Table 11. ^c (96 ± 1/2)% anhydrous N₂H₄. ^d Original temperature units in K. Converted to °C in third column. Ahlert et al.'s data were used as *saturated-liquid density* by Das and Kuloor [68-das/kul] to estimate the saturated-liquid molar specific volume listed in Table 12.

equation to combine with $\rho_v^{\text{int}}(T)$ may introduce physical incompatibilities that impact directly the estimate of the specific volumes and, in turn, plague the determination of other properties, such as the vaporization enthalpy, for example. This rather important aspect seems to have been drastically overlooked [49-sco/oli, 59-mar, 65-haw/har, 68-das/kul]. There will be occasion to come back to it again in the following section in the course of the discussion about the Clausius–Clapeyron equation.

D. Enthalpy of Vaporization. The literature [34-hie/woe, 39-fre/kar, 41-gig, 49-sco/oli, 51-aud/ogg, 64-cha/gok, 68-das/kul, 84-sch] offers a rather shaky support relative to the vaporization enthalpy (or latent heat) of N₂H₄. A striking, and somewhat unexpected, feature perceived from the cited references is the lack of a genuinely experimental nature of the published data. They have all been unconditionally estimated via approximate methods; calorimetric determinations are absent, although their feasibility with modern techniques has been recognized [81-zem/dit]. Val-

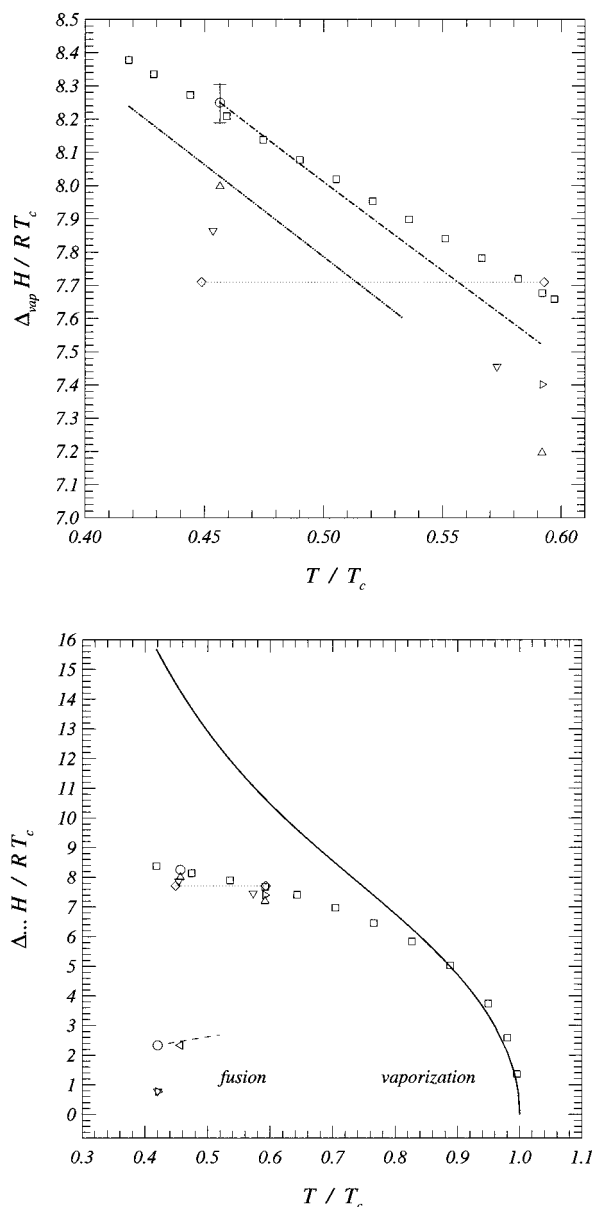


Figure 5. Vaporization enthalpy (a, top) below the NBP and (b, bottom) up to the critical point, and (b, bottom) fusion enthalpy in the vicinity of the NMP: ▽, Hieber and Woerner [34-hie/woe]; ◇···◇, Fresenius and Karweil [39-fre/kar]; right triangle, Giguere [41-gig]; ○, Scott et al. [49-sco/oli]; left triangle, Kit and Evered [60-kit/eve]; □, Das and Kuloor [68-das/kul]; △ Schmidt [84-sch]; - · - ·, interpolation (eq 14) by Audrieth and Ogg [51-aud/ogg]; - · · - ·, interpolation (eq 17) by Chang and Gokcen [64-cha/gok]; —, theoretical prediction according to Berthelot model [00-gio/des]; - - - -, interpolation (eq 24) by Audrieth and Ogg.

ues collected from [34-hie/woe, 39-fre/kar, 41-gig, 49-sco/oli, 84-sch] and [68-das/kul] are tabulated respectively in Tables 13 and 14 and compared in Figure 5. Those included in Table 13 have been surveyed by Audrieth and Ogg [51-aud/ogg], Kit and Evered [60-kit/eve], and Schmidt [84-sch]; Yaws et al. [74-yaw/hop] correlated Audrieth and Ogg's data, together with those of Scott et al. [49-sco/oli], according to the engineering formulas reviewed by Gambill [57-gam, 58-gam] and Li and Canjar [59-li/can], and presented the temperature dependence of the vaporization enthalpy in graphical form. Figure 5a evidences explicitly that almost all authors have confined themselves to give the enthalpy of vaporization for one or, at most, two temperatures, prudently far from the critical point. Differences

among the several estimates are evident. Das and Kuloor [68-das/kul] take exception from the other authors because, as illustrated in Figure 5b, their data cover the whole range of temperature from 273.16 K to 650 K, that is, practically up to the critical point.

The common characteristic of the data presented in Tables 13 and 14 is that they have all been systematically derived from the Clausius–Clapeyron equation

$$\frac{dp_v}{dT} = \frac{\Delta_{\text{vap}}H}{MT(v_v - v_l)} \quad (5)$$

appropriately complemented with (curve fits of) experimental vapor pressure data and more or less simplifying assumptions to allow the determination of the saturated-vapor and -liquid specific volumes.

Hieber and Woerner [34-hie/woe], and Fresenius and Karweil [39-fre/kar] based their estimate on the rather popular assumption of perfect-gas behavior of the vapor ($v_v \approx RT/p_vM$) in conjunction with the negligibility of the saturated-liquid specific volume ($v_v - v_l \approx v_v$). Such a simplification, although untenable in the neighborhood of the critical point ($T \rightarrow T_c$), brings eq 5 into the approximate form

$$d \ln p_v \approx \frac{\Delta_{\text{vap}}H}{RT^2} dT = -\frac{\Delta_{\text{vap}}H}{R} d\frac{1}{T} \quad (6)$$

Hieber and Woerner opted for the integration of eq 6 in temperature intervals sufficiently small to justify the negligibility of the temperature dependence of the vaporization enthalpy ($\Delta_{\text{vap}}H = \text{constant}$); with this provision, the latter quantity could, then, be obtained at once from

$$\Delta_{\text{vap}}H \approx R \frac{T_1 T_2}{T_2 - T_1} \ln \frac{p_{v2}}{p_{v1}} \quad (7)$$

for the temperature $(T_2 + T_1)/2$, with the aid of the experimental data listed in Table 5. In particular, they selected the data marked with an asterisk in Table 5 and obtained the two vaporization enthalpy values listed in Table 13. The reason of such a choice is not evident from their paper. In this regard, raising a word of warning about the subtleties lurking behind the use of eq 7 is compelling. There are two factors involved: one is the experimental error affecting temperature and vapor pressure measured data; the other is the *a priori* unawareness concerning the consistency of the temperature intervals, at which vapor pressure measurements were carried out, with the assumption of negligible variations of the vaporization enthalpy. Their interplay can lead to unpredictable results. For example, following Hieber and Woerner's method, the selection of the data in rows 3 and 4 (original units) of Table 5 implies $\Delta t = 23.73 - 23.67 = 0.06$ °C, an apparently small interval, but the application of eq 7 yields, at $t = (23.73 + 23.67)/2 = 23.7$ °C, a temperature sufficiently near to the 23.1 °C produced by Hieber and Woerner's selection, an unrealistically high vaporization enthalpy of 46.7 kcal·mol⁻¹. These considerations warn even more severely against the approach of Fresenius and Karweil, who, trusting the seemingly rigorous linearity of their vapor pressure curve (see Figure 2a), rearranged eq 6 into the form

$$\Delta_{\text{vap}}H \approx -R \frac{d \ln p_v}{d(1/T)} \approx R \cdot \text{constant} \quad (8)$$

and, from the slope of their graph, obtained a constant

vaporization enthalpy of 10 000 cal·mol⁻¹ (41 868 J·mol⁻¹) (see Table 13) in the range from 20 °C (293.15 K) up to their experimentally found NBP, fixed at 113.40 °C (386.55 K) (see Table 4).

Scott et al. did not assume a perfect-gas behavior of the vapor. They relied on the Berthelot state equation to describe the liquid and vapor phases of N₂H₄ and used the critical data from de Bruyn [96-deb] to determine the two constants required in such a state equation. They, then, employed the following least-squares fit

$$\log_{10} p_v/\text{mmHg} = 7.80687 - 1680.745/(t + 227.74) \quad (9)$$

of their measured vapor pressure data with the double purpose of (a) obtaining the saturated-vapor and -liquid specific volumes, by combining eq 9 with the assumed state equation, and (b) providing the derivative on the left-hand side of eq 5. Following this method, their calculation gave a vaporization enthalpy of $(10\,700 \pm 75)$ cal·mol⁻¹ ($44\,798.76 \pm 314.10$ J·mol⁻¹) (see Table 13) at 298.15 K. However, the accuracy of this estimate appears questionable when cross-examined against the curve (solid line in Figure 5b) generated from a rigorously theoretical calculation [00-gio/des] of the vaporization enthalpy corresponding to the thermodynamic model based on the Berthelot state equation. The huge discrepancy between the theoretical prediction (solid line) and Scott et al.'s estimate (circle) suggests the existence of a physical inconsistency between eq 9 and the Berthelot state equation that invalidates the use of the latter; it also represents an outstanding example of the potential conflict, already remarked upon at the end of Section 2.C, introduced by the combination of an arbitrarily chosen theoretical state equation with an interpolating function of experimental vapor pressure data. The approach followed by Das and Kuloor is very similar to the one of Scott et al. They obtained the derivative on the left-hand side of eq 5 from eq 1 and used the saturated-liquid and -vapor specific volumes tabulated in Table 12. Calculation methods, imprecisions, and inaccuracies connected with the latter data have been pointed out and discussed more specifically in Section 2.C. At any rate, Das and Kuloor produced the most plentiful series of vaporization enthalpy data (Table 14); these appear consistent with those listed in Table 13 and present the correct behavior in the vicinity of the critical point (see Figure 5b). Schmidt also conformed to the method of Scott et al. and Das and Kuloor to derive his vaporization enthalpy data; however, this author adopted his own curve fit of vapor pressure data from [34-hie/woe, 49-sco/oli, 64-cha/gok] but did not declare explicitly how the determination of the saturated-vapor and -liquid specific volumes was dealt with in his calculation.

As a complement to tabulated data, Audrieth and Ogg [51-aud/ogg] and Chang and Gokcen [64-cha/gok] have provided analytical expressions (dash-dot and dash-dot-dot lines in Figure 5a, respectively) of the vaporization enthalpy as a function of temperature. Audrieth and Ogg based their derivation on the implied, but not stated, assumption that (what they claimed to be) the Kirchhoff law could be applied to vaporization; in other words, they posed

$$\Delta_{\text{vap}}H(T) - \Delta_{\text{vap}}H(298.16\text{ K}) \approx \int_{298.16\text{ K}}^T (C_{p,v} - C_{p,l}) dT \quad (10)$$

and relinquished the contribution

$$I = M \int_{298.16\text{ K}}^T [v_v(1 - \alpha_v T) - v_l(1 - \alpha_l T)] \frac{dp_v}{dT} dT \quad (11)$$

Table 19. Solid Density Data Measured by Various Authors

source	ref	original units		SI units	
		$t/^\circ\text{C}$	$\rho/(\text{g}\cdot\text{cm}^{-3})$	T/K	$10^{-3}\rho/(\text{kg}\cdot\text{m}^{-3})$
Beck	43-bec	-5.0	1.146	268.15	1.146
Chang et al.	76-cha/pos	-30.0	1.2052	243.15	1.2052
		-30.0	1.2073	243.15	1.2073
		-20.0	1.2009	253.15	1.2009
		-20.0	1.2027	253.15	1.2027
		-4.5	1.1891	268.65	1.1891
		-4.2	1.1894	268.95	1.1894

Table 20. Experimental Pressure–Volume–Temperature Data Obtained by Giguere and Rundle [41-gig/run]

original units				SI units			
$t/^\circ\text{C}$	p/mmHg	V/cm^3	m/g	T/K	$10^{-4}p/\text{Pa}$	$10^6V/\text{m}^3$	$10^3m/\text{kg}$
90	265	213	0.0778	363.15	3.53	213	0.0778
95	273	213	0.0778	368.15	3.64	213	0.0778
100	277	213	0.0778	373.15	3.69	213	0.0778
110	287	213	0.0778	383.15	3.83	213	0.0778
120	294	213	0.0778	393.15	3.92	213	0.0778
131	747	220	0.2090	404.15	9.96	220	0.2090

that would make eq 10 exact if added to its right-hand side. In eq 11, $\alpha = 1/v(\partial v/\partial T)_p$ represents the coefficient of thermal expansion or expansivity. More exact differential forms of eq 10 and associated simplifications have been thoroughly discussed by Planck [22-pla] and Denbigh [81-den] and, concerning sublimation, by Zemansky [81-zem/dit]. Neglecting the contribution I turns out to be an acceptable approximation for N_2H_4 under the circumstance that its saturated vapor behaves like a perfect gas ($\alpha = 1/T$). Indeed, the quantity $(1 - \alpha_v T)$ undoubtedly vanishes in that case. Concerning the liquid ($\alpha \sim 10^{-4} \text{K}^{-1}$), the factor $\alpha_l T$ can be safely neglected with respect to unity even up to the critical point ($T = T_c = 653.15 \text{K}^{-1}$). With these provisions, the integral in eq 11 reduces to

$$I \approx -M \int_{p_v(298.16\text{K})}^{p_v(T)} v_l dp_v \quad (12)$$

Taking into account the weak variability of the saturated-liquid specific volume, a fair estimate of the order of magnitude is simply

$$|I| \sim M v_c [p_v(T) - p_v(298.16 \text{K})] \approx (4 \times 10^{-3}) M [p_v(T) - 1.917 \times 10^3] \quad (13)$$

In eq 13, v_c and $p_v(298.16 \text{K})$ are taken from Tables 1 and 6, respectively. At the NBP [$p_v(T_{\text{NBP}}) = 1.01325 \times 10^5 \text{Pa}$], one finds $|I| \sim 13 \text{J}\cdot\text{mol}^{-1}$, a rather negligible amount when compared to the order of magnitude of the data tabulated in Tables 13 and 14. Audrieth and Ogg complemented eq 10 with the enthalpy of vaporization supplied by Scott et al. [49-sco/oli] [$\Delta_{\text{vap}}H(298.16 \text{K}) = 10700 \text{cal}\cdot\text{mol}^{-1}$ (44798.76 $\text{J}\cdot\text{mol}^{-1}$)] and with interpolation polynomials for the constant-pressure heat capacities of saturated vapor and liquid, also constructed on data calculated and measured by Scott et al., although the latter data do not correspond rigorously to saturation conditions (see Section 7 and Tables 26 and 27). The final expression reads (sic)

$$\Delta_{\text{vap}}H/(\text{cal}\cdot\text{mol}^{-1}) = 15879 - 28.296T + 0.054525T^2 - 0.000068528T^3 + 0.0000003125T^4 - 0.0000000008333T^5 \quad (14)$$

and is understood to be valid in the temperature range from

25 °C to 66 °C (298.16 K to 340 K), according to information deduced from Audrieth and Ogg's text. Curiously enough, the authors misused eq 14 outside its range of validity to find a vaporization enthalpy of 9760 $\text{cal}\cdot\text{mol}^{-1}$ (40863.17 $\text{J}\cdot\text{mol}^{-1}$) at the NBP. Chang and Gokcen also relied on eq 10 for their derivation of the vaporization enthalpy. In addition, they assumed constant the difference between the constant-pressure heat capacities and set the values of the latter to those given at 298.16 K by Scott et al. (see Tables 26 and 27). With $C_{p,v} - C_{p,l} = \Delta C_p \approx 12.6 - 23.62 \approx -11.02 \text{cal}\cdot\text{mol}^{-1}\cdot\text{K}^{-1}$ ($-46.14 \text{J}\cdot\text{mol}^{-1}\cdot\text{K}^{-1}$), eq 10 becomes a linear function of temperature

$$\Delta_{\text{vap}}H(T) = \Delta_{\text{vap}}H(298.16 \text{K}) - 298.16\Delta C_p + T\Delta C_p \quad (15)$$

ΔH_0^{in} , in the notation of [64-cha/gok]

that allows to integrate eq 6 as

$$\ln p_v = \frac{\Delta C_p}{R} \ln T - \frac{\Delta H_0^{\text{in}}}{T} + \text{constant} \quad (16)$$

Chang and Gokcen derived the parameter ΔH_0^{in} and the integration constant from a least-squares fit of eq 16 on the base of their vapor pressure experimental data (see Table 8) and obtained the final expression (sic)

$$\Delta_{\text{vap}}H/(\text{cal}\cdot\text{mol}^{-1}) = 13691 - 11.00T \quad (17)$$

valid in the temperature range from 2.9 °C to 51.47 °C (276.05 K to 324.62 K). From eq 17, Chang and Gokcen evaluated $\Delta_{\text{vap}}H(298.16 \text{K}) = 10411 \text{cal}\cdot\text{mol}^{-1}$ (43588.77 $\text{J}\cdot\text{mol}^{-1}$).

The foregoing survey should sufficiently consolidate the impression expressed at the beginning of this section: available vaporization enthalpy data do not possess a sufficient degree of experimental *purity*. Their reliability could be potentially deteriorated by overlooked inconsistencies and/or unverified inaccuracies. Moreover, an additional danger of data-quality degradation lies concealed behind the derivative on the left-hand side of eq 5. In this regard, the author certainly subscribes to the following appropriate admonition of Reid et al. [87-rei/pr]: "An element of uncertainty is introduced in using any analytical vapor pressure–temperature equation to obtain accurate values of slopes dP_{vp}/dT . The constants in the equation may be optimum for correlating vapor pressures, but it does not necessarily follow that these same constants give the best fit for computing slopes" (see page 219 of [87-rei/pr]; P_{vp} corresponds to p_v).

3. Solid–Liquid Saturation Curve

The solid–liquid saturation curve has received much less attention than the liquid–vapor counterpart; as a matter of fact, the sole parameter that has been repeatedly measured during the course of the years is the normal melting point (NMP) [95-deb-1, 95-deb-2, 96-cur, 96-deb, 23-fri, 34-hie/woe, 38-sem, 39-fre/kar, 40-ple, 41-gig, 49-sco/oli, 49-moh/aud, 73-wil, 78-lit/mis, 85-han, 87-rei/pr]. The data are collected in Table 15, and most of them have been surveyed in [51-aud/ogg, 84-sch]. The values range between 1 °C and 2.2 °C (274.15 K and 275.35 K) (see Figure 6), and the agreement among the various authors is not as tight as in the case of the NBP.

Concerning the variation of the NMP with pressure, Hoffman [76-hof] seems to have been the only researcher to investigate experimentally the solid–liquid saturation

Table 21. Sound Speed and Compressibility Coefficients of Liquid N₂H₄ at 25 °C (298.15 K)

source	ref	original units			γ	SI units	
		$a_L/(\text{m}\cdot\text{s}^{-1})$	$10^6\kappa_T/(\text{cm}^2\cdot\text{kg}^{-1})$	$10^6\kappa_T/(\text{cm}^2\cdot\text{kg}^{-1})$		$10^{11}\kappa_T/\text{Pa}^{-1}$	$10^{11}\kappa_T/\text{Pa}^{-1}$
Thompson and Parsons	47-tho/par			25.4 ^a			25.90
Kretschmar	53-kre	2059 ^b					
Kretschmar	54-kre	2090	22.36	24.83	1.11	22.80	25.32
		2090	22.36	24.38	1.09	22.80	24.86
Kretschmar	55-kre	2069 ^c					

^a Taken from Chang et al. [76-cha/pos] and Schmidt [84-sch]. Corresponding temperature not explicitly given. Considered of low reliability by Schmidt. ^b Accuracy of $\pm 6 \text{ m}\cdot\text{s}^{-1}$. Sample of 96% N₂H₄. ^c Calculated from interpolation formula.

Table 22. Coefficient of Isothermal Compressibility^a of Solid N₂H₄ Measured by Chang et al. [76-cha/pos]

$t/^\circ\text{C}$	original units		SI units	
	κ_T/atm^{-1}		T/K	κ_T/Pa^{-1}
-30.0	↑		243.15	↑
-20.0	10×10^{-5}		253.15	9.9×10^{-10}
-4.2	↓		268.95	↓

^a Average over different measured values, according to the authors.

Table 23. Constant-Volume Molar Heat Capacity of N₂H₄ Vapor Measured and Estimated by Fresenius and Karweil [39-fre/kar]; $p = 10^{-4} \text{ mmHg}$ ($1.33 \times 10^{-2} \text{ Pa}$)

$t/^\circ\text{C}$	original units		SI units		
	$C_V/(\text{cal}\cdot\text{mol}^{-1}\cdot\text{K}^{-1})$		T/K	$C_V/(\text{J}\cdot\text{mol}^{-1}\cdot\text{K}^{-1})$	
	calc	meas			
40	9.65	9.6	313.15	40.40	40.2
67	10.38	10.4	340.15	43.46	43.5

Table 24. Constant-Volume Molar Heat Capacity of N₂H₄ Vapor Measured by Eucken and Krome [40-euc/kro]; $p = 6 \times 10^{-4} \text{ mmHg}$ ($8.00 \times 10^{-2} \text{ Pa}$)

T/K	original units		SI units	
	$C_V/(\text{cal}\cdot\text{mol}^{-1}\cdot\text{K}^{-1})$		$C_V/(\text{J}\cdot\text{mol}^{-1}\cdot\text{K}^{-1})$	
212	20.2		84.6	
287	11.2		46.9	
315	9.6		40.2	
341	10.4		43.5	

curve through a series of repeated tests; his data are listed in Table 16 and shown in Figure 6. Hoffman attempted also a theoretical prediction of the saturation curve based on the integration of the applicable Clausius–Clapeyron equation

$$\frac{dp_1}{dT} = \frac{\Delta_{\text{fus}}H}{MT(v_1 - v_s)} \quad (18)$$

under the assumption of constant ratio $\Delta_{\text{fus}}H/(v_1 - v_s)$. The latter quantity was evaluated in a rather approximate manner from the enthalpy of fusion $\Delta_{\text{fus}}H(274.56 \text{ K}) = 3025 \text{ cal}\cdot\text{mol}^{-1}$ ($12\,665 \text{ J}\cdot\text{mol}^{-1}$) provided by Scott et al. [49-sco/oli] (see Table 17) but admittedly declared inaccurate by these authors, from the liquid density $\rho(273.15 \text{ K}, p = ?) = 1.025 \text{ g}\cdot\text{cm}^{-3}$ ($1.025 \times 10^3 \text{ kg}\cdot\text{m}^{-3}$) measured by Walden and Hilgert [33-wal/hil] (see Table 18), and from the solid density $\rho(268.15 \text{ K}, p = ?) = 1.146 \text{ g}\cdot\text{cm}^{-3}$ ($1.146 \times 10^3 \text{ kg}\cdot\text{m}^{-3}$) determined by Beck [43- bec] (see Table 19). With proper conversion of units, the integration of eq 18 yielded

$$T = T_{\text{NMP}} \exp\left[\frac{(p_1/\text{psi}) - 14.7}{5.56 \times 10^5}\right] \quad (19)$$

but given the approximations mentioned above, the range

Table 25. Constant-Pressure Molar Heat Capacity of Solid N₂H₄ Measured by Scott et al. [49-sco/oli]

T/K	original units		SI units	
	$C_p/\text{cal}\cdot\text{mol}^{-1}\cdot\text{K}^{-1}$	$C_p/\text{J}\cdot\text{mol}^{-1}\cdot\text{K}^{-1}$	T/K	$C_p/\text{cal}\cdot\text{mol}^{-1}\cdot\text{K}^{-1}$
12	0.070	0.293	90	6.720
13	0.095	0.398	95	7.060
14	0.115	0.481	100	7.375
15	0.140	0.586	110	7.980
16	0.165	0.691	120	8.540
17	0.205	0.858	130	9.070
18	0.250	1.047	140	9.570
19	0.300	1.256	150	10.045
20	0.350	1.465	160	10.600
25	0.680	2.847	170	10.935
30	1.105	4.626	180	11.360
35	1.605	6.720	190	11.775
40	2.130	8.918	200	12.195
45	2.675	11.20	210 ^a	12.610
50	3.215	13.46	220	13.030
55	3.740	15.66	230	13.445
60	4.230	17.71	240	13.865
65	4.700	19.68	250	14.280
70	5.145	21.54	260	14.700
75	5.560	23.28	270	15.120
80	5.965	24.97	274.69 ^a	15.310
85	6.355	26.61		64.100

^a Data in this temperature range were extrapolated.

Table 26. Constant-Pressure Molar Heat Capacity of Liquid N₂H₄ Measured by Scott et al. [49-sco/oli]

T/K	original units		SI units	
	$C_p/(\text{cal}\cdot\text{mol}^{-1}\cdot\text{K}^{-1})$		$C_p/(\text{J}\cdot\text{mol}^{-1}\cdot\text{K}^{-1})$	
274.69	23.29		97.51	
280	23.37		97.85	
290	23.51		98.43	
298.16	23.62		98.89	
300	23.65		99.02	
310	23.80		99.65	
320	23.96		100.3	
330	24.14		101.1	
340	24.34		101.9	

of validity of this expression remains unidentified. The saturation curve generated from eq 19 with the NMP assumed by Hoffman at 35.6 °F (275.15 K) is drawn in Figure 6 (dash-dot line) and does not match the experimental data. The reason adduced by the author to explain the displacement between theoretical prediction and experimental results was the presence of water in the N₂H₄ sample used in the experiment, which reduced its purity to about 98%. Equation 19 was also reported by Schmidt [84-sch], who, however, used bars as pressure units and, accordingly, presented the argument of the exponential factor as $[(p_1/\text{bar}) - 1]/(3.8 \times 10^4)$.

Another expression for the melting-point increase with pressure valid in the vicinity of the NMP was proposed by Chang et al. [76-cha/pos]. They expanded linearly satura-

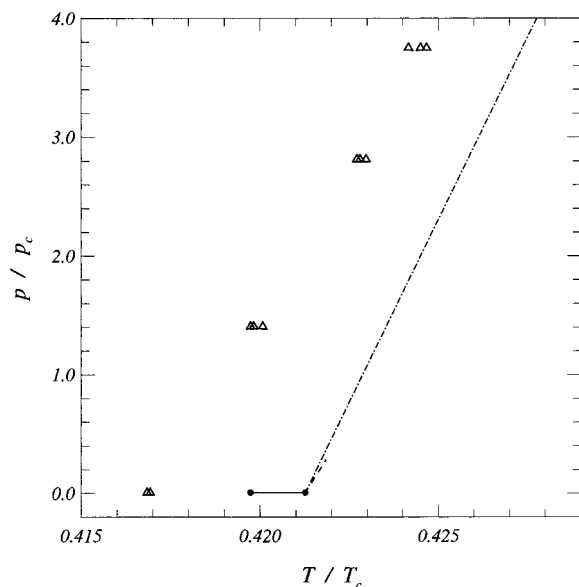


Figure 6. Experimental and theoretical solid–liquid saturation curve: ●–●, NMP experimental range from Table 15; Δ, Hoffman [76-hof]; - - -, integration of the Clausius–Clapeyron equation (eq 19) by Hoffman; - · - ·, NMP–vicinity linear expansion (eq 22) by Chang et al. [76-cha/pos].

Table 27. Constant-Pressure Molar Heat Capacity of N₂H₄ Vapor Calculated by Scott et al. [49-sco/oli]

original units		SI units	original units		SI units
<i>T</i>	<i>C_p</i>	<i>C_p</i>	<i>T</i>	<i>C_p</i>	<i>C_p</i>
K	(cal·mol ⁻¹ ·K ⁻¹)	(J·mol ⁻¹ ·K ⁻¹)	K	(cal·mol ⁻¹ ·K ⁻¹)	(J·mol ⁻¹ ·K ⁻¹)
298.16	12.6	52.8	900	21.5	90.0
300	12.6	52.8	1000	22.3	93.4
400	15.1	63.2	1100	23.1	96.7
500	16.9	70.8	1200	23.9	100
600	18.3	76.6	1300	24.5	103
700	19.5	81.6	1400	25.1	105
800	20.6	86.2	1500	25.5	107

tion pressure versus temperature

$$p_1 \approx p_1(T_{\text{NMP}}) + (T - T_{\text{NMP}}) \left(\frac{dp_1}{dT} \right)_{\text{NMP}} \quad (20)$$

and set the NMP to 2 °C (275.15 K) [95-deb-1, 49-moh/aud] together with $p_1(T_{\text{NMP}})$ atm. Then, they evaluated the saturation-pressure slope from the right-hand side of eq 18 according to the following simplifications: the enthalpy of fusion was taken equal to the previously indicated value given by Scott et al. at 274.56 K, and the saturated specific volumes were estimated from the liquid density calculated at $t = 2$ °C via their interpolating function

$$\rho/(\text{g}\cdot\text{mL}^{-1}) = 1.02492 - 0.000865t \quad (21)$$

and from the solid density calculated at the same temperature from eq 27. Following such approximations and with proper unit conversions, the final expression reads

$$\frac{T - 275.15}{(p_1/\text{atm}) - 1} = \frac{\Delta T}{\Delta p} = 0.00945 \text{ K}\cdot\text{atm}^{-1} \quad (22)$$

As illustrated in Figure 6 (dashed line), eq 22 agrees well with eq 19 in the vicinity of the NMP.

The enthalpy of fusion is another property related to the saturation curve for which a few data are available. These are tabulated in Table 17 and shown in Figure 5b. The

value provided by Hieber and Woerner [34-hie/woe] is the only one of truly experimental nature. The value given by Giguere [41-gig] agrees well with the former, but its experimental character remains unknown. The enthalpy of fusion estimated by Scott et al. is admittedly declared, by the authors themselves, affected by large uncertainties caused by the arbitrary extrapolation of the solid constant-pressure heat capacity in the vicinity of the NMP. Concerning the value taken from the collection of Kit and Evered [60-kit/eve], it is not possible to assess its reliability and original source due to lack of specific information.

Following the same method applied for the vaporization enthalpy (see Section 2.D), Audrieth and Ogg [51-aud/ogg] derived an analytical expression for the enthalpy of fusion from the approximate Kirchhoff law

$$\Delta_{\text{fus}}H(T) - \Delta_{\text{fus}}H(274.56 \text{ K}) \approx \int_{274.56 \text{ K}}^T (C_{p,l} - C_{p,s}) dT \quad (23)$$

supplemented with the enthalpy of fusion given by Scott et al. at 274.56 K and with their interpolation polynomials for the constant-pressure heat capacities (see Section 7). The final expression reads

$$\Delta_{\text{fus}}H/(\text{cal}\cdot\text{mol}^{-1}) = -732 + 20.836T - 0.0318T^2 + 0.00002033T^3 \quad (24)$$

and is understood to apply up to ~67 °C (340.15 K); the corresponding curve is shown in Figure 5b (dashed line). However, the reader is warned that eq 24 is potentially affected by inaccuracies. Indeed, apart from the fact, already pointed out in Section 2.D, that Audrieth and Ogg's heat capacity polynomials are constructed on Scott et al.'s measured data which do not correspond rigorously to saturation conditions, the polynomial relative to the solid-phase heat capacity substituted by the authors in the integrand of eq 23 turned out to be not applicable in the temperature range of integration.

4. Solid–Vapor Saturation Curve

Data relative to the solid–vapor saturation curve are basically nonexistent. The literature offers only the single value 2.60 mmHg (3.47×10^2 Pa) for the saturation pressure of the vapor in contact with the solid phase measured at 0 °C (273.15 K) by Scott et al. [49-sco/oli].

Giguere and Rundle [41-gig/run] and, subsequently, Kit and Evered [60-kit/eve] reported a sublimation enthalpy of 11.0 kcal·mol⁻¹ (46.0 kJ·mol⁻¹). The origin of this value, however, is uncertain because Giguere and Rundle claimed to have taken it from the experimental paper of Hieber and Woerner [34-hie/woe] but careful inspection of [34-hie/woe] reveals no trace of such a value.

5. Density

The earliest determinations of N₂H₄ liquid density trace back to the experiences of de Bruyn [95-deb-1, 95-deb-2, 96-deb], Brühl [97-bru], and Dito [02-dit]. Successive measurements were carried out by Walden and Hilgert [33-wal/hil], Barrick et al. [36-bar/dra], Semishin [38-sem], Hough et al. [50-hou/mas], Kretschmar [53-kre, 54-kre], Ahlert et al. [62-ahl/bau], and Laachach et al. [92-laa/fer]. The experimental data published by the mentioned authors, with the exception of Kretschmar's and Laachach et al.'s, have also been collected in the compilations of [51-aud/ogg, 60-kit/eve, 76-hof, 84-sch]; Yaws et al. [74-yaw/hop] presented in graphical form the data tabulated by Audrieth and Ogg [51-aud/ogg]. A single liquid-density

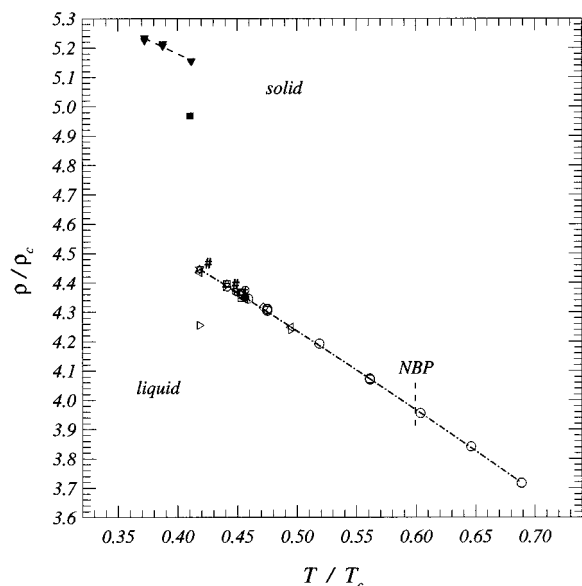


Figure 7. Liquid- and solid-density: \square , de Bruyn [95-deb-1, 95-deb-2, 96-deb]; ∇ , Brühl [97-bru]; \emptyset , Dito [02-dit]; \triangle , Walden and Hilgert [33wal/hil]; \diamond , Barrick et al. [36-bar/dra]; left triangle, Semishin [38-sem]; \blacksquare , Beck [43-pec]; right triangle, Hough et al. [50-hou/mas]; \oplus , Kretschmar [53-kre, 54-kre]; \circ , Ahlert et al. [62-ahl/bau]; \blacktriangledown , Chang et al. [76-cha/pos]; \otimes , Hannum [85-han]; $\#$, Laachach et al. [92-laa/fer]; $- \cdot -$, interpolation (eq 25) by Ahlert et al. [62-ahl/bau]; $- - -$, interpolation (eq 27) by Chang et al. [76-cha/pos].

value is present in the manual published by Hannum [85-han], but its experimental nature could not be ascertained. Table 18 contains the data in question, and Figure 7 illustrates how they compare with each other. The data appear consistent and, generally, in substantial agreement; only the measurement at 0 °C (273.15 K, $T/T_c \approx 0.42$) of Hough et al. diverges noticeably from those of the other authors. The slight difference between the two measurements of Kretschmar could probably be explained by the lesser purity, 96% according to the author, of the N_2H_4 used in the tests described in [53-kre]. The reader is referred to Section 2.C for details concerning misinterpretations of the described data as corresponding to saturated conditions.

The weak variability of liquid density with pressure is reflected in the attitude of the experimenters to omit considerations about the influence of the latter parameter; indeed, a common characteristic of most of the mentioned references is the lack of information regarding the pressure at which the measurements were taken. Only Hough et al. declare explicitly that their experiments were carried out under atmospheric pressure. Ahlert et al. also comment briefly about the evolution of the pressure during their experiments: they seem to indicate that their data correspond to different pressure levels, with a peak of 12 atm (1.2159×10^6 Pa) at 449.83 K (rightmost circle in Figure 7), but do not provide any more quantitative information in that regard. Their comment is somehow consistent with the location of the three experimental points at the right of the NBP in Figure 7. These points would represent metastable states if Ahlert et al.'s measurements were all rigorously taken at 1.01325×10^5 Pa; on the other hand, at 12 atm (1.2159×10^6 Pa) the boiling point, namely ~ 481 K ($T/T_c = 0.74$), lies well to the right of Ahlert et al.'s last experimental point, confirming, in so doing, the stable-state nature of all measurements taken by these authors.

Liquid-density interpolating functions have been provided by Walden and Hilgert [33-wal/hil], reported also in

[51-aud/ogg], Ahlert et al. [62-ahl/bau], Chang et al. [68-cha/gok], both surveyed in [84-sch], and Schmidt [84-sch]. The expression produced by Ahlert et al. (dash-dot line in Figure 7)

$$\rho/(\text{g}\cdot\text{cm}^{-3}) = 1.2471 - 0.07226(T/100) - 0.003191(T/100)^2 \quad (25)$$

allows satisfactory prediction in the whole temperature range of the available experimental data (see Table 18), but notwithstanding the authors' comment about pressure variations during their experiments, it also raises some questions of validity when the pressure becomes comparable with the critical one. The expression proposed by Schmidt

$$\rho/(\text{g}\cdot\text{cm}^{-3}) = 1.23078 - (6.2668 \times 10^{-4})T - (4.5284 \times 10^{-7})T^2 \quad (26)$$

is substantially equivalent to eq 25.

The situation relative to the density of solid N_2H_4 is much poorer than that of the liquid. Table 19 lists the very few available data; these are also shown in Figure 7 (solid symbols). The earliest experimental result was published by Beck [43-pec] in 1943; his single value can also be found in [51-aud/ogg, 60-kit/eve, 76-hof]. New experimental data came after a gap of 33 years through a series of experiments carried out by Chang et al. [76-cha/pos]; these authors least-squares fitted their data and provided the following interpolating expression (dashed line in Figure 7)

$$\rho/(\text{g}\cdot\text{mL}^{-1}) = 1.1869 - 0.000675t \quad (27)$$

which has also been reported in [84-sch]. The considerations regarding the influence of pressure mentioned previously apply here as well.

The pressure–volume–temperature measurements carried out by Giguere and Rundle [41-gig/run] constitute basically all that is available in the literature concerning the density of N_2H_4 in the vapor phase. Their experimental data, tabulated in Table 20, are relative to two samples of N_2H_4 with different mass; thus, the experimental points from 90 °C to 120 °C (363.15 K to 393.15 K) belong all to the isochor $\rho = 0.3653 \text{ kg}\cdot\text{m}^{-3}$ while the single test at 131 °C (404.15 K) corresponds to $\rho = 0.95 \text{ kg}\cdot\text{m}^{-3}$. Giguere and Rundle's data have been plotted for convenience in Figure 1 in connection with the misinterpretation of Kit and Evered [60-kit/eve] and Das and Kuloor [68-das/kul] (see Section 2.C), who erroneously assumed the data as corresponding to *saturated conditions*.

6. Speed of Sound and Compressibility Coefficients

Experimental work aimed to determine speed of sound and compressibility coefficients of liquid N_2H_4 was mainly carried out by Kretschmar [53-kre, 54-kre, 55-kre]. In a first experience [53-kre], the isentropic speed of sound $a_L = [-v^2(\partial p/\partial v)_s]^{1/2}$ was measured in an appreciably diluted (96%) sample, whereas, one year later [54-kre], the same physical variable was again measured in a purer sample together with the coefficient of isothermal compressibility $\kappa_T = -1/v(\partial v/\partial p)_T$ and density ρ (see Table 18); the coefficient of isentropic compressibility $\kappa_s = -1/v(\partial v/\partial p)_s$ and the heat capacity ratio followed respectively from the exact relations $\kappa_s = 1/\rho a_L^2$ and $\gamma = \kappa_T/\kappa_s$. Additional information regarding the isentropic speed of sound is available from

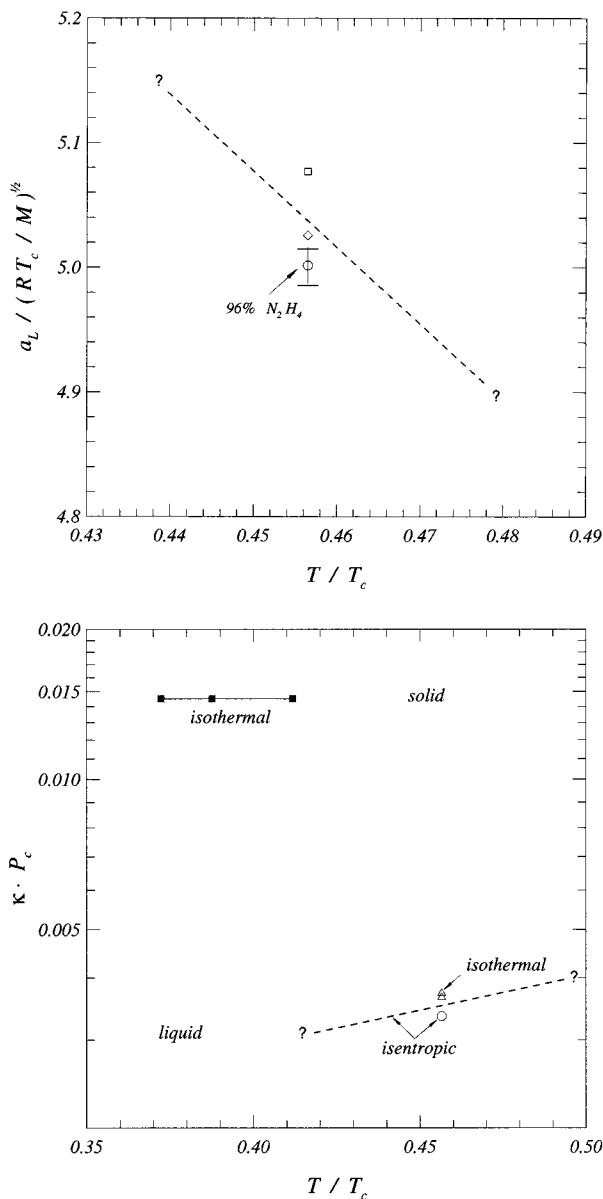


Figure 8. (a, top) Isentropic speed of sound in liquid N_2H_4 measured by Kretschmar (○, [53-kre]; □, [54-kre]; ◇, [55-kre]) with the interpolation (eq 28) by Schmidt [84-sch] (---). (b, bottom) Coefficients of isothermal compressibility: △, Kretschmar [54-kre] (liquid N_2H_4); ■—■, Chang et al. [76-cha/pos] (solid N_2H_4). Coefficients of isentropic compressibility: ○, Kretschmar [54-kre]; ---, interpolation (eq 29) by Schmidt [84-sch].

Kretschmar's experimental work [55-kre] with hydrazine–water mixtures. In [55-kre], the author proposed an interpolating expression, valid at 25 °C (298.15 K), as a function of the fractional weight of N_2H_4 which yields $a_L \approx 2069 \text{ m}\cdot\text{s}^{-1}$ for the pure compound, although the value mentioned in the text of the reference is 2074 $\text{m}\cdot\text{s}^{-1}$. Kretschmar's data are shown in Figure 8 and are listed in Table 21.

The experimental determination of the coefficient of isothermal compressibility of solid N_2H_4 was aimed at by Chang et al. [76-cha/pos]. Unfortunately, they were only able to provide an average value of $10 \times 10^{-5} \text{ atm}^{-1}$ ($0.987 \times 10^{-9} \text{ Pa}^{-1}$) (see Figure 8b and Table 22). These authors mention also a value of $2.54 \times 10^{-5} \text{ atm}^{-1}$ ($2.51 \times 10^{-10} \text{ Pa}^{-1}$) relative to liquid N_2H_4 and that they attributed to Thompson and Parsons [47-tho/par]; the reliability of such a value, however, was considered poor by Schmidt [84-sch].

The data published by Kretschmar and Chang et al. have been surveyed by Schmidt. However, Kretschmar's compressibility coefficients (see Table 21) have been reported with some minor imprecisions: a factor of 10^{-6} is missing in the values relative to the isothermal compressibilities, whereas the value for the isentropic compressibility is incorrectly indicated as $2.35 \times 10^{-5} \text{ cm}^2\cdot\text{kg}^{-1}$ ($2.39 \times 10^{-10} \text{ Pa}^{-1}$).

Schmidt proposed also interpolation expressions for the isentropic speed of sound

$$a_L / (\text{m}\cdot\text{s}^{-1}) = 3224.9 - 3.8611 T \quad (28)$$

and for the coefficient of isentropic compressibility

$$\kappa_s / (\text{Pa}^{-1}) = 1.2989 \times 10^{-10} - (4.6172 \times 10^{-13}) T + (2.7802 \times 10^{-15}) T^2 \quad (29)$$

Equation 29 is based on data attributed to rather unprocurable Rocketdyne reports. The dashed lines in Figure 8 illustrate the trend of eqs 28 and 29; the bounding question marks emphasize the lack of information relative to the temperature range of validity, which, unfortunately, was not explicitly given.

7. Heat Capacities

Fresenius and Karweil [39-fre/kar] and Eucken and Krome [40-euc/kro] were, apparently, the first experimenters that attempted N_2H_4 heat capacity measurements by determining the constant-volume heat capacity of the vapor phase at pressures as low as 10^{-4} mmHg and $6 \times 10^{-4} \text{ mmHg}$ ($1.33 \times 10^{-2} \text{ Pa}$ and $8.00 \times 10^{-2} \text{ Pa}$), respectively (see Figure 10 and Tables 23 and 24). Eucken and Krome's data at 315 K and 341 K are satisfactorily in agreement with those provided by Fresenius and Karweil at similar temperatures. The former authors aimed their attention also toward the low-temperature region and carried out measurements at 287 K and even at 212 K; Audrieth and Ogg [51-aud/ogg], however, have raised a warning concerning the doubtfulness of such measurements and their outcomes.

The first thorough experimental investigation came with the work of Scott et al. [49-sco/oli], which was given widespread diffusion through [51-aud/ogg, 54-kob/har, 60-kit/eve, 65-haw/har, 68-das/kul, 71-stu/pro, 74-yaw/hop, and 84-sch] and still retains today its role of primary reference. These authors were able to provide the constant-pressure heat capacity from 12 K to 1500 K, covering, in so doing, solid (Figure 9 and Table 25), liquid (Figure 9 and Table 26), and vapor (Figure 10 and Table 27) phases. The data relative to solid and liquid phases were obtained via calorimetric methods. The uncertainty of the values corresponding to solid N_2H_4 was claimed to be at most 0.3%, but curiously enough, it was considered not satisfactory (!) by the authors; no analogous information was given for the liquid. An important piece of information which, unfortunately, is missing is the pressure at which the experiments were carried out; on the other hand, the solid–liquid transition at the NMP (see Section 3) appearing in Table 1 of [49-sco/oli] seems to suggest that the pressure should have been 760 mmHg ($1.01325 \times 10^5 \text{ Pa}$). In this regard, a somewhat intriguing feature of the mentioned table is the presence of the label “sat” subscripting the symbol of the heat capacity, which, in the course of a hurried inspection, would definitely be interpreted as conveying the word saturation and mislead the reader to consider the data as corresponding to such conditions. This is exactly what was

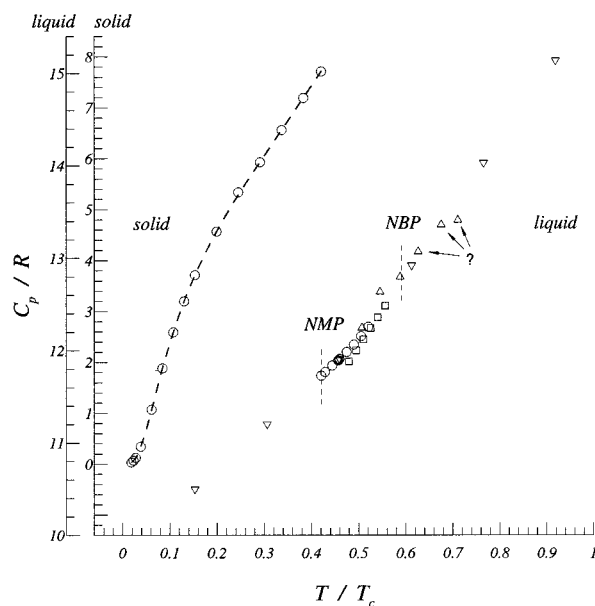


Figure 9. Constant-pressure heat capacity of solid and liquid N_2H_4 : \circ , Scott et al. [49-sco/oli]; \square , Hough et al. [50-hou/mas]; \diamond , Wagmann [64wag]; \triangle , Ahlert and Younts [68-ahl/you] (97% commercial N_2H_4); ∇ , JANAF Tables [71-stu/pro] (linearly extrapolated from Scott et al.'s data); ---, interpolation (eq 30) by Audrieth and Ogg [51-aud/ogg].

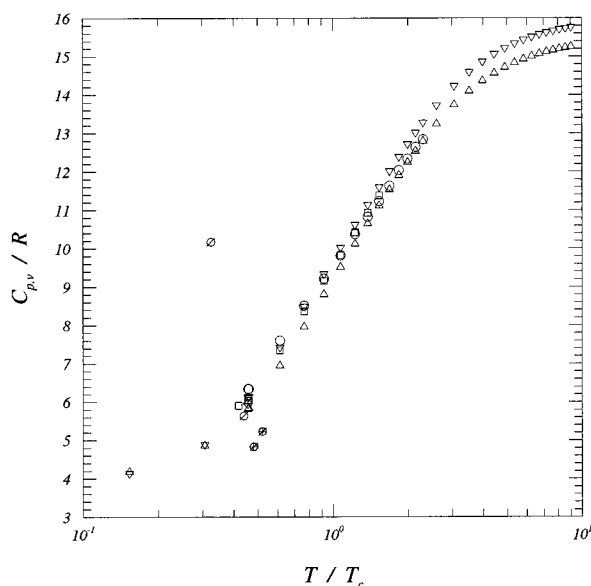


Figure 10. Constant-pressure heat capacity of N_2H_4 vapor: \circ , Scott et al. [49-sco/oli]; \diamond , Wagmann [64-wag]; \square , Haws and Harden [65-haw/har]; ∇ , JANAF Tables [71-stu/pro]; \triangle , Gurvich et al. [89-gur/vey]. Constant-volume heat capacity data from Fresenius and Karweil [39-fre/kar] [\oplus , $p = 10^{-4}$ mmHg (1.33×10^{-2} Pa)] and Eucken and Krome [40-euc/kro] [\otimes , $p = 6 \times 10^{-4}$ mmHg (8.00×10^{-2} Pa)] are also shown.

done by Audrieth and Ogg [51-aud/ogg] and by Chang and Gokcen [64-cha/gok] when they used the data of Tables 26 and 27 to derive the vaporization enthalpy as a function of temperature (see Section 2.D and eqs 14 and 17, respectively); Audrieth and Ogg systematically repeated the procedure with the data of Tables 25 and 26 for the derivation of the enthalpy of fusion (see Section 3 and eq 24). With concern to heat capacity data misuse, the following remark of Schmidt [84-sch] appears rather appropriate: "The heat capacity is a function of the pressure, and results would be different if measurements were

Table 28. Constant-Pressure Heat Capacity of Liquid N_2H_4 Measured by Hough et al. [50-hou/mas]

$t/^\circ\text{C}$	original units		SI units	
	$c_p/(\text{cal}\cdot\text{g}^{-1}\cdot^\circ\text{C}^{-1})$	T/K	$c_p/(\text{J}\cdot\text{kg}^{-1}\cdot\text{K}^{-1})$	
40	0.7368	313.15	3085	
50	0.7443	323.15	3116	
60	0.7517	333.15	3147	
70	0.7593	343.15	3179	
80	0.7665	353.15	3209	
90	0.7742	363.15	3241	

Table 29. Constant-Pressure Molar Heat Capacity of Liquid and Vapor N_2H_4 from Wagman [64-wag]

T/K	$C_p/(\text{J}\cdot\text{mol}^{-1}\cdot\text{K}^{-1})$	
	liq	vap
298.15	98.87	49.58

Table 30. Constant-Pressure Heat Capacity of N_2H_4 Vapor Estimated by Haws and Harden [65-haw/har] by Averaging Data from Fricke [48-fri] and from Scott et al. [49-sco/oli]

$t/^\circ\text{F}$	original units		SI units	
	$c_p/(\text{Btu}\cdot\text{lbm}^{-1}\cdot\text{R}^{-1})$	T/K	$c_p/(\text{J}\cdot\text{kg}^{-1}\cdot\text{K}^{-1})$	
32.0	0.3660	273.15	1532	
77.0	0.3746	298.15	1568	
80.6	0.3747	300.15	1569	
260.6	0.4554	400.15	1907	
440.6	0.5180	500.15	2169	
620.6	0.5674	600.15	2376	
800.6	0.6089	700.15	2549	
980.6	0.6459	800.15	2704	
1160.6	0.6772	900.15	2835	
1340.6	0.7052	1000.15	2953	

Table 31. Constant-Pressure Heat Capacity of Liquid N_2H_4 Measured by Ahlert and Younts [68-ahl/you]

$t/^\circ\text{C}$	original units		SI units		
	$c_p/(\text{cal}\cdot\text{g}^{-1}\cdot^\circ\text{C}^{-1})$		T/K	$c_p/(\text{J}\cdot\text{kg}^{-1}\cdot\text{K}^{-1})$	
	meas	corr			
58	0.786	0.759	331.15	3291	3178
83	0.811	0.783	356.15	3395	3278
111	0.822	0.793	384.15	3442	3320
136	0.839	0.810	409.15	3513	3391
168	0.858	0.828	441.15	3592	3467
191	0.863	0.831	464.15	3613	3479

conducted at saturation pressure or under truly isobaric conditions".

No other experimental determination of solid heat capacity has ever been attempted after Scott et al.'s investigation. For liquid N_2H_4 , instead, additional measurements were carried out by Hough et al. [50-hou/mas] (Table 28) and Ahlert and Younts [68-ahl/you] (Table 31), duly reported in [84-sch]. As illustrated in Figure 9, the data published by these authors slightly differ from those of Scott et al. in the temperature range bounded by the NMP and the NBP. Hough et al. performed experiments aimed to determine liquid density and constant-pressure heat capacity of the hydrazine-water system. It is not clear from their text if the atmospheric-pressure condition established during the liquid density experiments (see Section 5) was also secured in the heat capacity measurements. Ahlert and Younts, in turn, explicitly declared their data as representative of the standard state at 1 atm (1.01325×10^5 Pa). On the other hand, they worked with commercial N_2H_4 with a purity of 97% in weight and they adduce this fact as the explanatory justification for the vertical offset of their data shown in Figure 9. Moreover, the location at the right of the NBP of the last three

Table 32. Constant-Pressure Molar Heat Capacity of Liquid N₂H₄ Tabulated in the JANAF Tables [71-stu/pro]

T/K	original units	SI units
	$C_p/(\text{cal}\cdot\text{mol}^{-1}\cdot\text{K}^{-1})$	$C_p/(\text{J}\cdot\text{mol}^{-1}\cdot\text{K}^{-1})$
100	20.850	87.295
200	22.250	93.156
298	23.623*	98.905
300	23.650*	99.018
400	25.660	107.43
500	27.860	116.64
600	30.060	125.86

Ahlert and Younts' experimental points, indicated with a question mark in Figure 9, remains unexplained. A conjecture based on the ebullioscopic increase due to the 3% water is untenable. Indeed, a rapid estimate from the boiling point curve of the hydrazine–water system provided by de Bruyn and Dito [02-deb/dit] would yield an NBP shift of about 4 K for a composition of 95% N₂H₄: such a shift cannot even accommodate the position of Ahlert and Younts' first experimental point to the right of the NBP shown in Figure 9, which corresponds to pure N₂H₄. One should conclude, therefore, that the experimental points in question represent metastable states, with the obvious hesitation arising from the doubtfulness of performing accurate measurements under such circumstances. Ahlert and Younts, however, do not say anything in this regard. More liquid N₂H₄ heat capacity data are reported in the *JANAF Tables* [71-stu/pro] (see Table 32): they include two experimental points from those of Scott et al., marked with an asterisk in Table 32, and other values that were obtained from those two by linear extrapolation. As shown in Figure 9, these data also trespass the NMP and NBP boundaries and their significance is open to question.

The data of Scott et al. relative to the vapor phase were calculated from spectroscopic data and molecular structure constants via partition function methods; in this sense, the data should be considered as corresponding to *perfect-gas* conditions and not truly experimental. This consideration applies also to the results presented by Fresenius and Karweil [39-fre/kar] as well as to the calculations reported in the *JANAF Tables* [71-stu/pro] and in the tables edited by Gurvich et al. [89-gur/vey]. The various data sets are compared in Figure 10. Some differences are evident and can be traced to differences in energy levels and molecular constants used in the partition function summations. Scott et al.'s data seem to agree with those of the *JANAF Tables* at low temperature but converge toward those of Gurvich et al. when the temperature increases. The data of Haws and Harden [65-haw/har] (Table 30) have been included because they were obtained by averaging Scott et al.'s data together with older data published by Fricke [48-fri] that are not easily accessible.

Interpolation functions for analytical calculations of the constant-pressure heat capacity have been provided in [51-aud/ogg, 54-kob/har, 65-haw/har, 68-das/kul, 68-ahl/you, 84-sch, and 87-rei/pra]. Audrieth and Ogg [51-aud/ogg] fitted the whole set of data published by Scott et al. [49-sco/oli] according to the polynomial expression

$$C_p/(\text{cal}\cdot\text{mol}^{-1}\cdot\text{K}^{-1}) = \sum_{k=0}^4 a_k T^k \quad (30)$$

The coefficients a_k in eq 30 are collected in Table 33. The accuracy of their polynomials is illustrated, for the solid phase, by the dashed line in Figure 9. Ahlert and Younts [68-ahl/you] and Schmidt [84-sch] supplied additional

interpolating expressions for the liquid phase. The former authors least-squares fitted their own data and proposed the linear expression

$$c_p/(\text{cal}\cdot\text{g}^{-1}\cdot^\circ\text{C}^{-1}) = 0.734 + (5.33 \times 10^{-4})t \quad (31)$$

Equation 31 has been reported by Schmidt with the temperature units misinterpreted as Kelvin rather than Celsius degrees. The latter author reports also the expression

$$c_p/(\text{cal}\cdot\text{g}^{-1}\cdot\text{K}^{-1}) = 0.29512 + (2.0193 \times 10^{-3})T - (1.8859 \times 10^{-6})T^2 \quad (32)$$

as an alternative to eq 31 but without specifying the originating source. However, the differences between eqs 31 and 32 are minor. Another expression

$$c_p/(\text{cal}\cdot\text{g}^{-1}\cdot\text{K}^{-1}) = 0.88415 - (1.3949 \times 10^{-3})T + (3.0074 \times 10^{-6})T^2 \quad (33)$$

was obtained by Schmidt by curve-fitting a combination of the data sets of Scott et al. and Hough et al. [50-hou/mas], respectively. As pertains the vapor phase, the interpolating functions suggested in [54-kob/har, 68-das/kul, and 87-rei/pra] are substantially equivalent to the corresponding polynomials of Audrieth and Ogg [51-aud/ogg]. On the other hand, the expression

$$c_p/(\text{Btu}\cdot\text{lbm}^{-1}\cdot\text{R}^{-1}) = 0.137857 + (0.052715 \times 10^{-3})T - (0.119907 \times 10^{-6})T^2 \quad (34)$$

given by Haws and Harden [65-haw/har], and reported as such in [84-sch], turns out to be affected by mistakes of unidentifiable nature. In particular, the temperature units on the right-hand side of eq 34 remain unknown: although Schmidt maintains that they are Kelvin degrees, in Table 3 of their paper Haws and Harden inconsistently use $\text{Btu}\cdot\text{lbm}^{-1}\cdot\text{R}^{-1}$ for the constant-pressure heat capacity and Fahrenheit degrees for temperature. At any rate, and contrary to the claim of the authors, eq 34 does not reproduce the values tabulated in the third column of their Table 3 whatever unit combination is adopted. Given these uncertainties, the use of eq 34 is strongly discouraged.

8. Enthalpy, Entropy, and Gibbs Energy

Truly experimental values for characteristic thermodynamic functions such as enthalpy, entropy, and Gibbs energy do not exist in the literature, and the available data are merely results of calculations based on more or less exact methods. Scott et al. [49-sco/oli] published the first set of data, listed in Table 34, for the vapor phase in the temperature range between 298.16 and 1500 K according to the partition function method already mentioned in Section 7; in this respect, their data reflect a perfect-gas connotation which makes them applicable only when the vapor phase behaves accordingly. Subsequent tabulations similarly based on the partition function method were provided in the *JANAF Tables* [71-stu/pro] and by Gurvich et al. [89-gur/vey] in the extended temperature range from 100 K to 6000 K. The data are compared in Figure 11b, Figure 12b, and Figure 13b and are found in satisfactory agreement; minor differences in the rightmost neighborhood of the temperature range can be traced to differences in the number of energetic levels accounted for in the sum-over-states of the partition function and in the numerical

Table 33. Polynomial Coefficients Provided by Audrieth and Ogg [51-aud/ogg] for Eq 30

temp range/K	$a_0/(\text{cal}\cdot\text{K}^{-1})$	$a_1/(\text{cal}\cdot\text{K}^{-2})$	$a_2/(\text{cal}\cdot\text{K}^{-3})$	$a_3/(\text{cal}\cdot\text{K}^{-4})$	$a_4/(\text{cal}\cdot\text{K}^{-5})$
			Solid		
12–25	0	0	0	0.000 042 8	0
25–60	0.374	–0.0674	0.003 93	–0.000 26/9	0
60–100	–3.194	0.1506	–0.000 45	0	0
100–170	–1.98	0.398/3	–0.000 475	0.000 002 5/3	0
170–274.69	3.833	0.0418	0	0	0
			Liquid		
274.69–340	24.696	–0.0218	0.000 061	0	0
			Vapor		
298.16–1000	–3.62	0.087 25	–0.000 433 75/3	0.000 000 125	–0.000 000 000 125/3
1000–1500	8.25	0.019	–0.000 005	0	0

values of the energies themselves. Gurvich et al. provided also the following curve-fits

$$\frac{H_{0\text{K}} - G^\circ}{T} = 2.420091 \times 10^2 + 1.630570 \times 10^1 \ln X - \frac{7.037611 \times 10^{-4}}{X^2} - \frac{8.010748 \times 10^{-2}}{X} + (6.656812 \times 10^2)X - (1.215491 \times 10^3)X^2 + (1.350379 \times 10^3)X^3 \quad (35)$$

$$\frac{H_{0\text{K}} - G^\circ}{T} = 4.397502 \times 10^2 + 1.072909 \times 10^2 \ln X - \frac{1.423171 \times 10^{-1}}{X^2} + \frac{7.595883}{X} + (5.139036 \times 10^1)X - (3.062831 \times 10^1)X^2 + 9.627167X^3 \quad (36)$$

for the standard-state Gibbs energy $G^\circ = G(T, p^\circ)$, in $\text{J}\cdot\text{mol}^{-1}$, as a function of the parameter $X = T/10000$ K. Equations 35 and 36 apply respectively in the temperature ranges below and above 1500 K, and, as illustrated by the dash-dot line in Figure 13b, match the discrete data very satisfactorily. For completeness, it ought to be remarked that the standard-state reference pressure assumed by Gurvich et al. is $p^\circ = 10^5$ Pa, whereas Scott et al.'s and *JANAF Tables'* data are relative to $p^\circ = 1.01325 \times 10^5$ Pa. This slightly different convention, however, bears little significance for the numerical data.

Figures 11b and 12b show also enthalpy and entropy predicted by the theoretical model developed by Das and Kuloor [68-das/kul], which is a slight modification of the one proposed by Haws and Harden [65-haw/har], based on a virial-expansion state equation. The enthalpy data lie systematically above the perfect-gas counterparts regardless of the pressure, a sign indicating a possible physical inconsistency affecting the state equation on which the model was constructed. On the contrary, the entropy data embed the perfect-gas ones and match them very accurately in correspondence of the standard pressure. Notwithstanding the well-behaved trend of the entropy, the ill-behaved trend featured by the enthalpy remains unexplained and makes questionable the validation of Das and Kuloor's and Haws and Harden's theoretical models.

The sole, and rather modest, tabulation relative to the liquid phase is contained in the *JANAF Tables* [71-stu/pro]; the corresponding data are shown in Figures 11a, 12a, and 13a. The information given in the tables concerning the methods used to obtain the data is extremely synthetic and not clearly detailed. The integration of the constant-pressure heat capacities listed in Table 32 and discussed in Section 7 seems to have played a role; but of course, the doubts already expressed therein concerning significance

Table 34. Molar Enthalpy, Entropy, and Gibbs Energy of N_2H_4 Vapor (Perfect-Gas) Calculated by Scott et al. [49-sco/oli]

Enthalpy and Entropy				
original units			SI units	
T	$H - H_{0\text{K}}$	S°	$H - H_{0\text{K}}$	S°
K	$\text{kcal}\cdot\text{mol}^{-1}$	$\text{cal}\cdot\text{mol}^{-1}\cdot\text{K}^{-1}$	$\text{J}\cdot\text{mol}^{-1}$	$\text{J}\cdot\text{mol}^{-1}\cdot\text{K}^{-1}$
298.16	2.812	57.41	11 773	240.4
300	2.835	57.49	11 870	240.7
400	4.221	61.46	17 672	257.3
500	5.823	65.03	24 380	272.3
600	7.584	68.23	31 753	285.7
700	9.482	71.16	39 699	297.9
800	11.48	73.83	48 064	309.1
900	13.59	76.31	56 899	319.5
1000	15.78	78.62	66 068	329.2
1100	18.06	80.79	75 614	338.3
1200	20.41	82.83	85 453	346.8
1300	22.83	84.77	95 585	354.9
1400	25.31	86.60	105 968	362.6
1500	27.80	88.35	116 393	369.9

Gibb's Energy		
original units		SI units
T	$(H_{0\text{K}} - G^\circ)/T$	$(H_{0\text{K}} - G^\circ)/T$
K	$\text{cal}\cdot\text{mol}^{-1}\cdot\text{K}^{-1}$	$\text{J}\cdot\text{mol}^{-1}\cdot\text{K}^{-1}$
298.16	47.98	200.9
300	48.04	201.1
400	50.91	213.1
500	53.39	223.5
600	55.59	232.7
700	57.61	241.2
800	59.47	249.0
900	61.21	256.3
1000	62.84	263.1
1100	64.37	269.5
1200	65.83	275.6
1300	67.21	281.4
1400	68.53	286.9
1500	69.80	292.2

of values exceeding the NMP and NBP boundaries apply here as well.

The integration of Scott et al.'s constant-pressure heat capacities, interpolated according to the polynomials generated from eq 30, was also the way followed by Audrieth and Ogg [51-aud/ogg] to produce analytical expressions of enthalpy and entropy, for solid, liquid, and vapor phases, and of Gibbs energy, for liquid and vapor phases only, versus temperature. Such expressions are too lengthy and involved to be reproduced here, and the interested reader is referred to the original reference. The dashed lines shown in Figures 11–13 have been obtained from the interpolating expressions in question. Not much can be said about the solid phase because of the lack of comparable data from other sources. Concerning the liquid phase, the curves

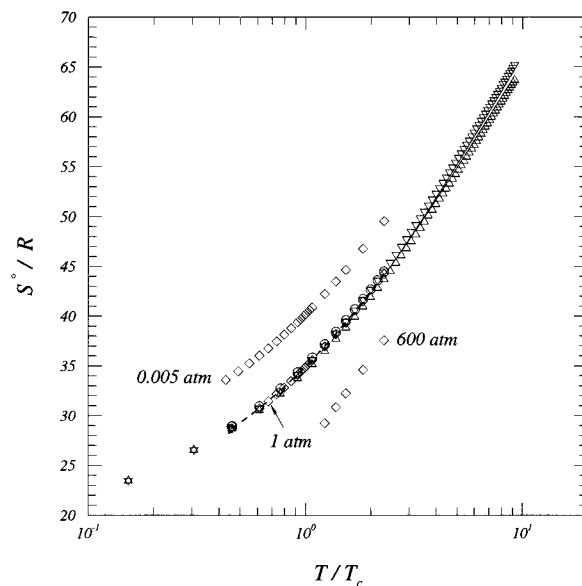
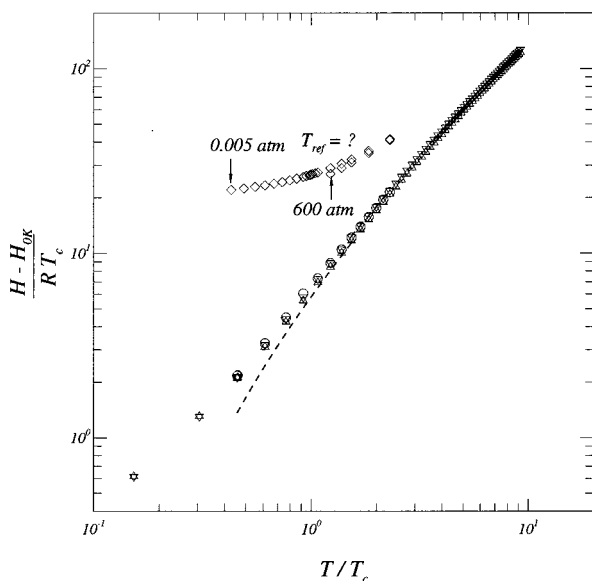
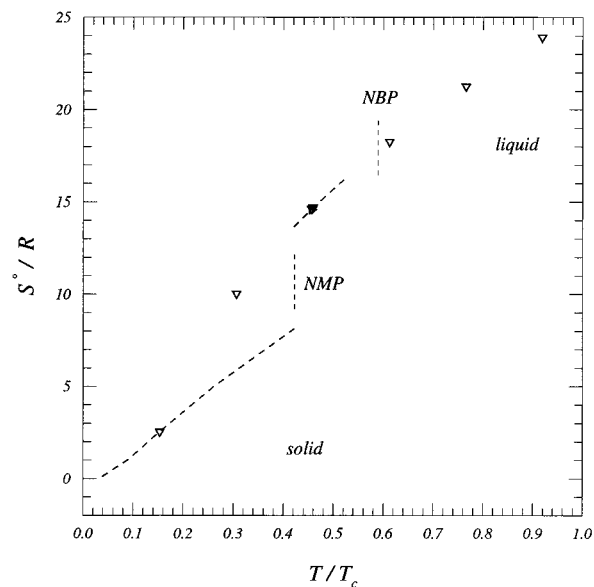
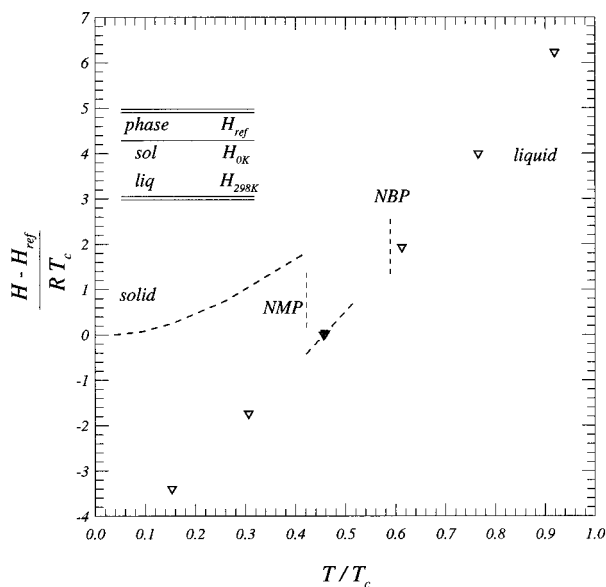


Figure 11. (a, top) Enthalpy of solid and liquid N_2H_4 : ∇ , *JANAF Tables* [71-stu/pro]; ---, interpolation by Audrieth and Ogg [51-aud/ogg]. (b, bottom) Enthalpy of N_2H_4 vapor (perfect gas): \circ , Scott et al. [49-sco/oli]; \diamond , Das and Kuloor [68-das/kul] (real gas); ∇ , *JANAF Tables* [71-stu/pro]; \triangle , Gurvich et al. [89-gur/vey]; ---, interpolation by Audrieth and Ogg [51-aud/ogg].

appear expectedly consistent with the data listed in the *JANAF Tables*, given the similarity of the methods; moreover, they remain coherently confined within the NMP and NBP boundaries. Audrieth and Ogg complemented the heat capacity integration with the usual enthalpies of vaporization $\Delta_{\text{vap}}H(298.16 \text{ K}) = 10\,700 \text{ cal}\cdot\text{mol}^{-1}$ ($44\,798.76 \text{ J}\cdot\text{mol}^{-1}$) and of fusion $\Delta_{\text{fus}}H(274.56 \text{ K}) = 3025 \text{ cal}\cdot\text{mol}^{-1}$ ($12\,665 \text{ J}\cdot\text{mol}^{-1}$) provided by Scott et al. (Tables 13 and 17). The inaccuracies of these values are pointed out in Sections 2.D and 3, and their effect becomes manifestly visible in the divergence of the dashed lines from the perfect-gas enthalpy and Gibbs energy data produced by Scott et al., *JANAF Tables*, and Gurvich et al. in Figures 11b and 13b.

9. Conclusions

The picture emerging from the considerations of the preceding sections surprisingly does not reveal the satisfac-

Figure 12. (a, top) Entropy of solid and liquid: right triangle, Wagmann [64-wag]; ∇ , *JANAF Tables* [71-stu/pro]; ---, interpolation by Audrieth and Ogg [51-aud/ogg]. (b, bottom) Entropy of N_2H_4 vapor (perfect gas): \circ , Scott et al. [49-sco/oli]; right triangle, Wagmann [64-wag]; \diamond , Das and Kuloor [68-das/kul] (real gas); ∇ , *JANAF Tables* [71-stu/pro]; \triangle , Gurvich et al. [89-gur/vey]; ---, interpolation by Audrieth and Ogg [51-aud/ogg].

tory situation intuitively expected for a compound such as N_2H_4 , which has found extensive use for many years as a propellant in the propulsion-engineering domain. The surprise is partially attenuated by taking into account that much attention has been mainly devoted to its performance as a fuel in relation to the design of thrusters for spacecraft attitude control or orbit adjustment; within that perspective, only products of N_2H_4 decomposition, typically N_2 , H_2 , and NH_3 , have to be dealt with and, in the vast majority of the cases, they can be satisfactorily assimilated to perfect gases. Nevertheless, applications involving potential phase changes, such as N_2H_4 flow in feeding and/or venting lines of propulsion subsystems, have to rely on rather shaky and insufficient support from the literature. Apart from minor concerns, some properties are certainly well investigated: examples are the vapor pressure of the saturated liquid, at least below the NBP, the liquid density, the heat

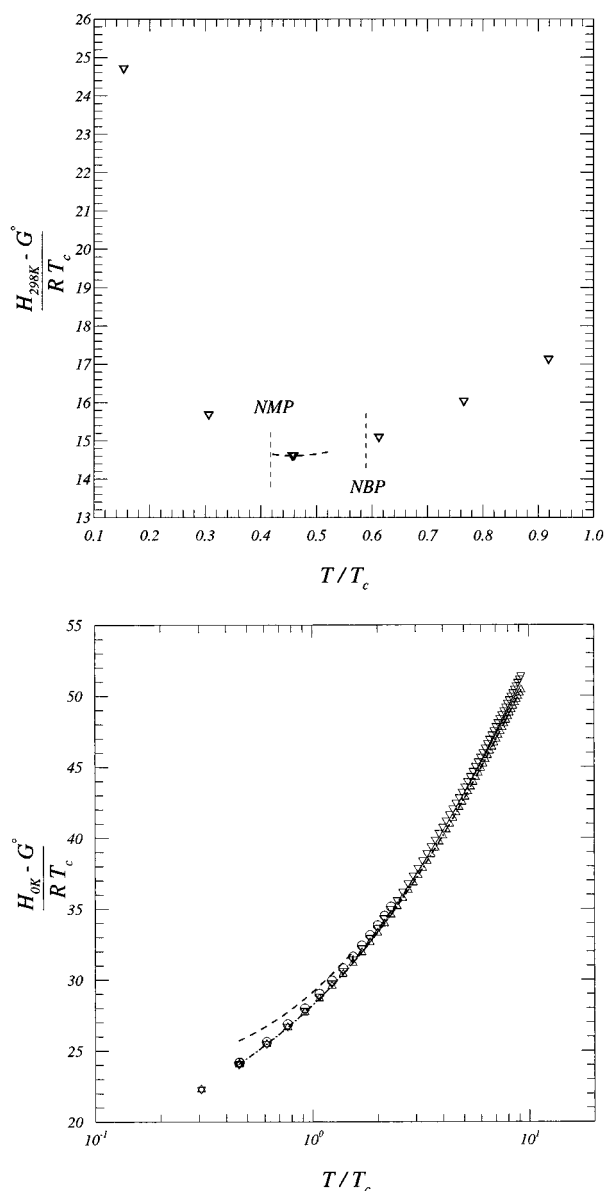


Figure 13. (a, top) Gibbs energy of liquid N_2H_4 : ∇ , *JANAF Tables* [71-stu/pro]; - - -, interpolation by Audrieth and Ogg [51-aud/ogg]. (b, bottom) Gibbs energy of N_2H_4 vapor (perfect gas): \circ , Scott et al. [49-sco/oli]; ∇ , *JANAF Tables* [71-stu/pro]; \triangle , Gurvich et al. [89-gur/vey]; - - -, interpolation by Audrieth and Ogg [51-aud/ogg]; - · -, interpolation (eqs 35 and 36) by Gurvich et al.

capacities, and the thermodynamic functions enthalpy, entropy, and Gibbs energy of the vapor phase when it behaves as a perfect gas. On the other hand, there are important properties for which the data are either lacking or old, scant, of unreliable source, inaccurate, and, worst of all, wrongly believed experimental in nature. The critical data, the saturation pressure relative to the solid-liquid and solid-vapor curves, the specific volumes (density) corresponding to saturation conditions, the phase-change enthalpies, the solid density, speed of sound, and compressibility coefficients, and the real-gas characteristics of the vapor phase can without hesitation be included in this category. Obvious recommendations ensuing from these remarks are to be always aware of the outlined limitations and hidden inaccuracies and to be on guard by exercising extreme prudence before hurriedly drawing conclusions when dealing with the data in question for the purpose of validating theoretical models. Within a more general

perspective, a necessary concern must be emphasized that arises when the weaknesses of the mentioned thermodynamic properties are confronted with the recognized existence of engineering problems that demand the knowledge of accurate data. Two typical examples, based on the author's experience, are the heater-failure related freezing of N_2H_4 in satellite tanks during operational life with the potential risk of pipe failure during the thawing process, and the venting of liquid N_2H_4 into empty space with the potential risk of pipe clogging due to solidification, either directly from liquid or following evaporation. They are connected with the accurate knowledge of the properties associated with, respectively, the solid-liquid and solid-vapor saturation curves, two zones of the (T, p) plane in which the data available today are either poor (the former) or completely absent (the latter).

In light of the foregoing considerations, the recognition of the need to improve the knowledge of the thermodynamic properties of N_2H_4 available today appears inescapable and constitutes strong motivation that justifies the procurement of more reliable, *truly* experimental values via supposedly more modern and refined measurement techniques complemented with rigorous support from theoretical thermodynamics.

Acknowledgment

The author wishes to acknowledge the assistance of R. Schwane and I. Kaelsch provided for the translation of excerpts from the German references, the availability of L. Marraffa to discuss different aspects involved in this work and his valuable suggestions, the help of T. Erickson for the final revision of the manuscript and check of the data included in the tables, and the efficient support provided by the ESTEC library staff, B. Cusveller in particular, for the timely procurement of the many bibliographic references required by this work.

List of Symbols

Variables

- a_L = isentropic speed of sound (Laplace characteristic velocity)
- a_k = polynomial coefficients for heat capacity interpolation
- C = heat capacity
- c = heat capacity (mass)
- G = Gibbs energy
- H = enthalpy
- $\Delta...H$ = phase-change enthalpy
- κ = compressibility coefficient
- M = N_2H_4 molar mass, $32.045\ 282 \times 10^{-3} \text{ kg}\cdot\text{mol}^{-1}$ (from Table 1 of [99-voc])
- m = mass
- p = thermodynamic pressure
- R = universal gas constant, $8.314\ 472 \text{ J}\cdot\text{mol}^{-1}\cdot\text{K}^{-1}$
- S = entropy
- T = thermodynamic temperature (K, unless otherwise indicated)
- t = Celsius temperature (unless otherwise indicated)
- v = specific volume (mass)
- X = $T/10000$ (in eqs 35 and 36)
- Z = compressibility factor
- α = coefficient of thermal expansion
- γ = heat capacity ratio
- ρ = density
- τ = reduced temperature

Sub/superscripts

c = critical

l = saturated liquid (in contact with vapor)

l = saturated liquid (in contact with solid)

p = constant-pressure

s = saturated solid

s = isentropic

T = isothermal

v = saturated vapor

v = constant-volume

° = standard state

Labels

fus = fusion

int = interpolated

the = theoretical

vap = vaporization

0 K = at $T = 0$ K298 K = at $T = 298.15$ K*Miscellaneous*

ln = logarithm to the base e

log₁₀ = logarithm to the base 10**Literature Cited**

- 86-cur/jay Curtius, T.; Jay, R. On Hydrazine. *Ber. Dtsch. Chem. Ges.* **1886**, 22R, 134–135 (in German).
- 93-cur Curtius, T. Studies on Hydrazine. *Ber. Dtsch. Chem. Ges.* **1893**, 26, 403–410 (in German).
- 94-deb Lobry de Bruyn, C. A. On Free Hydrazine (Diamide). *Recl. Trav. Chim.* **1894**, 13, 433–440 (in French).
- 95-deb Lobry de Bruyn, C. A. On Hydrazine Hydrate. *Recl. Trav. Chim.* **1895**, 14, 85–88 (in French).
- 95-deb-1 Lobry de Bruyn, C. A. Preparation Method and Features of Hydrazine. *Proc. K. Ned. Akad. Wet.* **1895**, 4, 73–74 (in Dutch).
- 95-deb-2 Lobry de Bruyn, C. A. On Free Hydrazine. *Ber. Dtsch. Chem. Ges.* **1895**, 28, 3085–3086 (in German).
- 96-cur Curtius, T. On Hydrazine, Nitrogen–Hydrogen, and Diazo-Compounds of the Fatty Series. *Ber. Dtsch. Chem. Ges.* **1896**, 29, 759–783 (in German).
- 96-deb Lobry de Bruyn, C. A. Free Hydrazine I. *Recl. Trav. Chim.* **1896**, 15, 174–184 (in French).
- 97-bru Brühl, J. W. Spectrochemistry of Nitrogen, V. Z. *Phys. Chem.* **1897**, 22, 373–409 (in German).
- 99-deb Lobry de Bruyn, C. A. On Free Hydrazine. *Recl. Trav. Chim.* **1899**, 18, 297–298 (in French).
- 02-dit Dito, J. W. The Densities of Mixtures of Hydrazine and Water. *Proc. K. Ned. Akad. Wet.* **1902**, 4, 756–758.
- 02-deb/dit Lobry de Bruyn, C. A.; Dito, J. W. The Boiling-Point Curve for the System: Hydrazine + Water. *Proc. K. Ned. Akad. Wet.* **1902**, 5, 171–174.
- 22-pla Planck, M. *Treatise on Thermodynamics*; Dover: New York, 1990 [Translated from the seventh German edition, 1922].
- 23-fri Friedrichs, F. Ammonates as Binary Systems. II. Hydrazine-Ammonia. *Z. Anorg. Allg. Chem.* **1923**, 127, 221–227 (in German).
- 33-wal/hil Walden, P.; Hilgert, H. Anhydrous Hydrazine as an Ionization Medium for Electrolytes and Nonelectrolytes. *Z. Phys. Chem.* **1933**, 165A, 241–271 (in German).
- 33-wes/hul West, C. J., Hull, C., Eds. *International Critical Tables of Numerical Data, Physics, Chemistry and Technology*; McGraw-Hill: New York, 1933; Vol. 3.
- 34-hie/woe Hieber, W.; Woerner, A. Thermochemical Measurements with Complex-Forming Amines and Alcohols. *Z. Elektrochem.* **1934**, 40, 252–256 (in German).
- 36-bar/dra Barrick, L. D.; Drake, G. W.; Lochte, H. L. The Parachor and Molecular Refraction of Hydrazine and some Aliphatic Derivatives. *J. Am. Chem. Soc.* **1936**, 58, 160–162.
- 38-sem Semishin, V. I. Internal Friction and Fusibility of the System Hydrazine-Water. *J. Gen. Chem. (USSR)* **1938**, 8, 654–661 (English summary).
- 39-fre/kar Fresenius, W.; Karweil, J. Normal Oscillations and Configuration of Hydrazine. II. The Ultrared Spectrum of Hydrazine. *Z. Phys. Chem.* **1939**, 44B, 1–13 (in German).
- 40-ple Pleskov, V. Ionization Product of Hydrazine. *Acta Physicochim. (USSR)* **1940**, 13, 662–676 (in Russian).
- 40-euc/kro Eucken, A.; Krome, H. The Implementation of the Thermal-Conductivity Method for the Measurement of the Molar Heat of Very Rarefied Gases by means of Simultaneous Determination of the Accommodation Coefficients. *Z. Phys. Chem.* **1940**, 45B, 175–192 (in German).
- 41-gig/run Giguere, P. A.; Rundle, R. E. The Vapour Density of Hydrazine. *J. Am. Chem. Soc.* **1941**, 63, 1135–1137.
- 41-gig Giguere, P. A. Spectroscopic Evidence of Hydrogen Bonds in Hydrogen Peroxide and Hydrazine. *Trans. R. Soc. Can.* **1941**, 35, 1–8.
- 43-bec Beck, G. On Special Properties of Carbohydrates, Amino acids and Hydrocarbons. *Wien. Chem.-Ztg.* **1943**, 46, 18–22 (in German).
- 44-her Herzog, R. Correlations of Critical Constants with Parachors. *Ind. Eng. Chem.* **1944**, 36, 997–1001.
- 47-tho/par Thompson, T.; Parsons, J. *Data on Properties and Manufacturing Methods for Anhydrous Hydrazine*; North American Aviation Report No. AL-275; Los Angeles, CA, 1947.
- 48-fri Fricke, E. *Cooling Equipment Design Study—The Thermodynamics of Oxygen, Hydrazine and Fluorine*; Republic Aviation Corp. Report No. F-5028-101; 1948.
- 49-sco/oli Scott, D.; Oliver, G.; Gross, M.; Hubbard, W.; Huffman, H. Hydrazine: Heat Capacity, Heats of Fusion and Vaporization, Vapor Pressure, Entropy and Thermodynamic Functions. *J. Am. Chem. Soc.* **1949**, 71, 2293–2297.
- 49-moh/aud Mohr, P.; Audrieth, L. F. The Hydrazine-Water System. *J. Phys. Colloid Chem.* **1949**, 53, 901–906.
- 50-hou/mas Hough, E. W.; Mason, D. M.; Sage, B. H. Heat Capacity of the Hydrazine-Water System. *J. Am. Chem. Soc.* **1950**, 72, 5774–5775.
- 51-aud/ogg Audrieth, L. F.; Ogg, B. A. *The Chemistry of Hydrazine*; John Wiley & Sons: New York, 1951.
- 52-bur Burtle, J. G. Vapour Pressure-Composition Measurements on Aqueous Hydrazine Solutions. *Ind. Eng. Chem.* **1952**, 44, 1675–1676.
- 53-kre Kretschmar, G. The Velocity of Sound in some Rocket Propellant Liquids. *ARS J.* **1953**, 23, 82–84.
- 54-kre Kretschmar, G. The Isothermal Compressibilities of some Rocket Propellant Liquids, and the Ratio of the two Specific Heats. *Jet Propul.* **1954**, 24, 175–186.
- 54-kob/har Kobe, K.; Harrison, R. Thermo Data for Petrochemicals. Part XXI. Ammonia, Hydrazine and the Methylamines. *Pet. Refin.* **1954**, 33, 161–164.
- 55-kre Kretschmar, G. Determination of the Velocity of Sound in Hydrazine-Water Mixtures by Means

- of the Debye-Sears Ultrasonic Light Diffraction Phenomenon. *J. Chem. Phys.* **1955**, *23*, 2102–2104.
- 55-mar/hou Martin, J. J.; Hou, Y. Development of an Equation of State for Gases. *AIChE J.* **1955**, *1*, 142–150.
- 57-gam Gambill, W. R. How to Estimate Engineering Properties—Latent Heat I. *Chem. Eng.* **1957**, *64*, 261–266.
- 58-gam Gambill, W. R. How to Estimate Engineering Properties—Latent Heat II. *Chem. Eng.* **1958**, *65*, 159–162.
- 59-li/can Li, C. C.; Canjar, L. N. Estimate Latent Heats Rapidly. *Pet. Refin.* **1959**, *38*, 233–235.
- 59-mar/kap Martin, J. J.; Kapoor, R. M.; De Nevers, N. An Improved Equation of State for Gases. *AIChE J.* **1959**, *5*, 159–160.
- 59-mar Martin, J. J. Correlations and Equations Used in Calculating the Thermodynamic Properties of Freon Refrigerants. In *Thermodynamics and Transport Properties of Gases, Liquids and Solids*; Touloukian, Y. S., Ed.; McGraw-Hill: New York, 1959; pp 110–122.
- 60-kit/eve Kit, B.; Evered, D. *Rocket Propellant Handbook*; Macmillan: New York, 1960.
- 62-ahl/bau Ahlert, R.; Bauerle, G.; Lecce, J. Density and Viscosity of Anhydrous Hydrazine at Elevated Temperatures. *J. Chem. Eng. Data* **1962**, *7*, 158–160.
- 63-pan/mig Pannetier, G.; Mignotte, P. Binary System Hydrazine-(Unsymmetrical Dimethylhydrazine) (I). Study of the Liquid–Vapor Equilibrium. *Bull. Soc. Chim. Fr.* **1963**, *130*, 694–698 (in French).
- 64-cha/gok Chang, E.; Gokcen, N. *Thermodynamic Properties of Hydrazine, Unsymmetrical Dimethylhydrazine, and their Mixtures*; Aerospace Corporation Report No. ATN-64(9228)-2; El Segundo, CA, 1964.
- 64-wag Wagman, D. Selected Values of Chemical Thermodynamic Properties. In *Proceedings of 2nd Meeting of ICRPG Working Group on Thermochemistry*; Chemical Propulsion Information Agency: Laurel, MD, 1964; p 13.
- 65-haw/har Haws, J. L.; Harden, D. G. Thermodynamic Properties of Hydrazine. *J. Spacecr. Rockets* **1965**, *2*, 972–974.
- 68-cha/gok Chang, E.; Gokcen, N.; Poston, T. Thermodynamic Properties of Gases in Propellants. II. Solubilities of Helium, Nitrogen, and Argon Gas in Hydrazine, Methylhydrazine, and Unsymmetrical Dimethylhydrazine. *J. Phys. Chem.* **1968**, *27*, 638–642.
- 68-das/kul Das, T. R.; Kuloor, N. R. Thermodynamic Properties of Hydrazine. *J. Ind. Inst. Sci.* **1968**, *50*, 13–25.
- 68-ahl/you Ahlert, R.; Younts, C. Heat Capacities of 90% Hydrogen Peroxide and Commercial Anhydrous Hydrazine. *J. Chem. Eng. Data* **1968**, *13*, 402–405.
- 71-stu/pro Stull, D.; Prophet, H. *JANAF Thermochemical Tables*; NSRDS-NBS-37; 1971.
- 73-mec Mechtly, E. A. *The International System of Units*; NASA SP-7012 (second revision); 1973.
- 73-wil Williams, L. *Hydrazine Purity Influence on Construction Material Compatibility*; AIAA paper 73-1264; 1973.
- 74-yaw/hop Yaws, C. L.; Hopper, J. R.; Rojas, M. G. Ammonia and Hydrazine. *Chem. Eng.* **1974**, *81*, 91–100.
- 76-hof Hoffman, R. T. *Deep Ocean Hydrazine Decomposition Testing*; Naval Undersea Center Report No. NUC TP 495; Kailua, HI, 1976.
- 76-cha/poc Chang, E.; Poston, T.; Gokcen, N. *Density, Compressibility, Thermal Conductivity, and Mechanical Movement of Solid Hydrazine*; Aerospace Corporation Report No. TR-0077(2409-01)-1; El Segundo, CA, 1976.
- 78-lit/mis Litvinova, L.; Mishchenko, K.; Kushchenko, V. Preparation of Pure Hydrazine by Directional Crystallization. *J. Appl. Chem. (USSR)* **1978**, *51*, 2491–2492.
- 81-den Denbigh, K. *The Principles of Chemical Equilibrium*; Cambridge University Press: Cambridge, 1993 [Reprinted from the fourth edition, 1981].
- 81-zem/dit Zemansky, M. W.; Dittman, R. H. *Heat and Thermodynamics*; McGraw-Hill: New York, 1981.
- 84-sch Schmidt, E. W. *Hydrazine and its Derivatives*; John Wiley & Sons: New York, 1984.
- 85-han Hannum, J. A. *Hazards of Chemical Rockets and Propellants. Volume 3: Liquid Propellants Manual*; Chem. Prop. Info. Agency Report No. AD-A158115; Laurel, MD, 1985.
- 87-rei/pri Reid, R.; Prausnitz, J.; Poling, B. *The Properties of Gases and Liquids*; McGraw-Hill: New York, 1987.
- 89-gur/vey Gurchich, L.; Veyts, I.; Alcock, C., Eds. *Thermodynamic Properties of Individual Substances*; Hemisphere Publishing Corporation: New York, 1989; Vol. 1, Part 2.
- 92-bel Bellajrou, R. Liquid–Vapor Equilibria. Application to the Ternary System $\text{NH}_3\text{--CH}_3\text{--NH}_2\text{--H}_2\text{O}$. Vapour Pressures and Decomposition Kinetics of N_2H_4 , $(\text{CH}_3)_2\text{NNH}_2$ and UH_25 . Ph.D. Thesis (30-92), Université Claude Bernard–Lyon I, 1992 (in French).
- 92-laa/fer Laachach, A.; Ferriol, M.; Cohen-Adad, M.-T.; Huck, J.; Jorat, L.; Noyel, G.; Getzen, F. W.; Bureau, J. C. Densities, Molar Volumes and Viscosities in the Systems Water–Hydrazine, Water–Methylhydrazine and Water–1,1-Dimethylhydrazine. *Fluid Phase Equilib.* **1992**, *71*, 301–312.
- 99-voc Vocke, R. D. Atomic Weights of the Elements 1997. *Pure Appl. Chem.* **1999**, *71*, 1593–1607.
- 00-gio/des Giordano, D.; De Serio, M. A Thermodynamic Model of Hydrazine that Accounts for Liquid–Vapor Phase Change. 35th AIAA Thermophysics Conference, 11–14 June 2001, Anaheim, CA (AIAA paper 2001–3016).

Received for review September 11, 2000. Accepted January 18, 2001.

JE0003010